

# Earth's Future



## RESEARCH ARTICLE

10.1029/2022EF002779

### Key Points:

- Erosion-rate is more strongly associated with temperature and vegetation than with wildfires, mass wasting and hydrologic conditions
- Erosion-rate meaningfully decreases with increased temperature, vegetation abundance, and relative abundance of trees and shrubs
- The association between erosion-rate to changes in climatic and environmental conditions is often threshold dependent

### Supporting Information:

Supporting Information may be found in the online version of this article.

### Correspondence to:

E. Shelef,  
[shelef@pitt.edu](mailto:shelef@pitt.edu)

### Citation:

Shelef, E., Griffore, M., Mark, S., Coleman, T., Wondolowski, N., Lasher, G. E., & Abbott, M. (2022). Sensitivity of erosion-rate in permafrost landscapes to changing climatic and environmental conditions based on lake sediments from Northwestern Alaska. *Earth's Future*, 10, e2022EF002779. <https://doi.org/10.1029/2022EF002779>

Received 18 MAR 2022

Accepted 24 JUN 2022

### Author Contributions:

**Conceptualization:** Eitan Shelef, Mark Abbott



**Data curation:** Melissa Griffore, Sam Mark, Nick Wondolowski, Mark Abbott

**Formal analysis:** Nick Wondolowski

**Funding acquisition:** Eitan Shelef, Mark Abbott

**Investigation:** Eitan Shelef, Melissa Griffore, Sam Mark, Tim Coleman, G. Everett Lasher, Mark Abbott

## Sensitivity of Erosion-Rate in Permafrost Landscapes to Changing Climatic and Environmental Conditions Based on Lake Sediments From Northwestern Alaska

Eitan Shelef<sup>1</sup> , Melissa Griffore<sup>1</sup>, Sam Mark<sup>1</sup> , Tim Coleman<sup>2</sup>, Nick Wondolowski<sup>1</sup>, G. Everett Lasher<sup>1</sup> , and Mark Abbott<sup>1</sup>

<sup>1</sup>Department of Geology and Environmental Science, University of Pittsburgh, Pittsburgh, PA, USA, <sup>2</sup>Marshall School of Business, University of Southern California, Los Angeles, CA, USA

**Abstract** Erosion of landscapes underlain by permafrost can transform sediment and nutrient fluxes, surface and subsurface hydrology, soil properties, and rates of permafrost thaw, thus changing ecosystems and carbon emissions in high latitude regions with potential implications for global climate. However, future rates of erosion and sediment transport are difficult to predict as they depend on complex interactions between climatic and environmental parameters such as temperature, precipitation, permafrost, vegetation, wildfires, and hydrology. Thus, despite the potential influence of erosion on the future of the Arctic and global systems, the relations between erosion-rate and these parameters, as well as their relative importance, remain largely unquantified. Here we quantify these relations based on a sedimentary record from Burial Lake, Alaska, one of the richest datasets of Arctic lake deposits. We apply a set of bi- and multi-variate techniques to explore the association between the flux of terrigenous sediments into the lake (a proxy for erosion-rate) and a variety of biogeochemical sedimentary proxies for paleoclimatic and environmental conditions over the past 25 cal ka BP. Our results show that erosion-rate is most strongly associated with temperature and vegetation proxies, and that erosion-rate decreases with increased temperature, pollen-counts, and abundance of pollen from shrubs and trees. Other proxies, such as those associated with fire frequency, aeolian dust supply, mass wasting and hydrologic conditions, play a secondary role. The marginal effects of the sedimentary-proxies on erosion-rate are often threshold dependent, highlighting the potential for strong non-linear changes in erosion in response to future changes in Arctic conditions.

**Plain Language Summary** Erosion of landscapes underlain by permafrost can transform arctic environments by changing topography, hydrology and rates of permafrost thaw. These changes can influence the entire arctic ecosystem as well as green house gas emissions from permafrost soils that can affect global climate. However, future rates of erosion are difficult to predict as they depend on complex interactions between climatic and environmental parameters such as temperature, permafrost, vegetation, wildfires, and hydrology. This complexity hinders assessments of the relations between erosion-rate and these parameters, and hence these relations as well as the relative importance of these different parameters remain largely unquantified. We used a lake sediment record as an archive for erosion from an upland Arctic watershed over the last 25,000 years. Results show that erosion-rate is most strongly associated with temperature and vegetation-related conditions, and that erosion-rate decreases with increase in temperature, pollen counts, and pollen-based proxy for the abundance of trees and shrubs increase. The effects of environmental conditions on erosion-rate often change abruptly across some threshold values, highlighting the potential for strong changes in erosion in response to future changes in Arctic conditions.

## 1. Introduction

Arctic environments are strongly affected by perturbations in climate, and their response may influence the global atmosphere and biosphere (e.g., Cohen et al., 2014; Natali et al., 2021; Schuur et al., 2008). The thawing of permafrost soils, for example, is projected to release vast amounts of organic carbon stored in permafrost soils to the atmosphere and induce a positive feedback between increasing temperature, thawing, and carbon release to the atmosphere (Harden et al., 2012; Schädel et al., 2016; Schuur et al., 2008; Turetsky et al., 2020; Zimov et al., 2006). Permafrost thaw can also increase rates of sediment transport and erosion through thermokarst expansion, reduced soil cohesion, and increased thickness of the active layer (the upper soil that thaws every summer)

© 2022 The Authors. Earth's Future published by Wiley Periodicals LLC on behalf of American Geophysical Union. This is an open access article under the terms of the [Creative Commons Attribution License](https://creativecommons.org/licenses/by/4.0/), which permits use, distribution and reproduction in any medium, provided the original work is properly cited.

**Methodology:** Eitan Shelef, Sam Mark, Tim Coleman

**Software:** Eitan Shelef

**Validation:** Tim Coleman, Mark Abbott

**Visualization:** Eitan Shelef

**Writing – original draft:** Eitan Shelef

**Writing – review & editing:** Melissa

Griffiore, Sam Mark, Tim Coleman, G.

Everett Lasher, Mark Abbott

(Kirkby, 1995; S. F. Lamoureux et al., 2014; Osterkamp et al., 2009; Olefeldt et al., 2016; Shelef et al., 2017; Toniolo et al., 2009; Turetsky et al., 2020). Increased rates of erosion and sediment transport can expose deep, frozen soils to a warm atmosphere and further expedite permafrost thaw and carbon release. Erosion can also change the surface topography and thus modify the distribution of solar radiation across the landscape and change surface and subsurface hydrology (e.g., Liljedahl et al., 2016; Turetsky et al., 2020; van Huissteden, 2020). Further, eroded soil particulates and nutrients transported into the Arctic aquatic systems (i.e., rivers, lakes, deltas, oceans) can degrade water quality (e.g., Bilotta & Brazier, 2008; Droppo et al., 2021; Levenstein et al., 2020), harm aquatic ecosystems (Chin et al., 2016; Vucic et al., 2020), and change the partitioning of carbon stocks between terrestrial and aquatic systems (Fuchs et al., 2020; Li et al., 2021; Rowland et al., 2010). Despite the potential influence of these processes on the Arctic system, the relations between erosion-rate and environmental conditions (e.g., climate, permafrost, vegetation, wildfires, hydrology) remain largely unquantified (Lane, 2012; Li et al., 2021; Pelletier et al., 2015; Rowland et al., 2010; Spencer & Lane, 2016), impeding predictions of the Arctic system's response to future changes.

The influence of future changes to the Arctic environment on rates and patterns of erosion and the resulting flux of sediments and carbon is a gap in our knowledge that is difficult to quantify and predict (Li et al., 2021; Rowland et al., 2010; Turetsky et al., 2019). Whereas erosion-rate typically increases with factors such as runoff, surface erodibility, and intensity of hillslope processes (e.g., freeze thaw, bioturbation, mass wasting), the influence of changes to the Arctic environment on these factors depend on complex and potentially counteractive interactions between temperature, permafrost, precipitation, vegetation, fire, and hydrology (Gooseff et al., 2009; Lara et al., 2019; Patton et al., 2019; Rowland et al., 2010). Climate warming, for example, may enhance permafrost thaw, causing a variety of thermokarst phenomena such as active layer detachment, retrogressive thaw slumps, and thermo-erosional gullies (Gooseff et al., 2009; Kokelj & Jorgenson, 2013; Lafrenière & Lamoureux, 2019; Lantz & Kokelj, 2008; Lewkowitz & Harris, 2005), and can act as a positive feedback for enhanced erosion along thawed ice wedges, water tracks, river banks and lake shores (Evans et al., 2020; Fuchs et al., 2020; Godin et al., 2014; Godin & Fortier, 2012; Trochim et al., 2016). Warming is also associated with lengthening of the growth season, increased vegetation cover, expansion of shrubs, and increased canopy height (Elmendorf et al., 2012; Myers-Smith et al., 2019). This can increase the thickness of winter snow drift trapped by vegetation which insulates the soil from cold winter temperatures, and enhance the protrusion of vegetation through snow that expedites spring snow melt, therefore causing further permafrost thaw (Domine et al., 2016; Wilcox et al., 2019) and associated erosion. Shrubs are associated with increased temperature of shallow soils (Kropp et al., 2020) and can also increase fire frequency through increased fuel supply (P. E. Higuera et al., 2008), enhancing fire-induced thaw and erosion-rate (Chipman & Hu, 2017; B. M. Jones et al., 2015; Patton et al., 2019).

Climate warming, however, can also reduce erosion-rate. For example, warming induced increase in vegetation cover and shrub expansion can stabilize the landscape through soil reinforcement and shielding by the root matrix and canopy, resulting in decreased erosion rates (Gyssels et al., 2005; S. Lamoureux, 2000; Tape et al., 2011). Further, thermal insulation by the root matrix and organic-rich topsoil (e.g., peat) together with the shading by shrubs can reduce the effect of a warming atmosphere on soil temperature, limiting permafrost thaw and associated erosion (Atchley et al., 2016; Mann et al., 2010; Yi et al., 2007). Warming can also increase the thickness of the active layer (Jorgenson et al., 2010; Lin & Wang, 2021; Romanovsky & Osterkamp, 1997), lowering the water table and increasing storage capacity, thus reducing surface runoff and erosion (Lamoureux, 2000; O'Connor et al., 2019; Woo, 1983) and suppressing the flashiness of erosive flows that occur at the end of cold springs (Cockburn & Lamoureux, 2008a; Woo & Sauriol, 1980). Overall, the counteractive erosive responses to interactions between climate, permafrost, vegetation and hydrology, demonstrate the complexity of the Arctic environment and have limited robust predictions of erosional response to changes in climate and environmental conditions.

Lake and river deposits preserve an integrated record of watershed response to past changes to the Arctic environment through biogeochemical sedimentary proxies for past erosion and environmental conditions, and thus may assist in modeling and quantifying the influence of environmental changes on erosion and sediment flux. For example, increased erosion at times of increased temperature is recorded by river deposits from the Bølling–Allerød (BA) and Holocene Thermal Maximum (HTM) warming events. High summer temperatures during these events (Gaglioti et al., 2014, 2017; Kaufman, 2004) were associated with extensive aggradation of river deposits in the northern foothills of Alaska, probably in response to increased sediment flux sourced from hillslope

erosion induced by permafrost thaw (Mann et al., 2002, 2010). Similarly, lake sediments in the Tanana Valley in central Alaska, and in the western Brooks Range (Abbott et al., 2000; Finkenbinder et al., 2014; Finkenbinder et al., 2015) record increased sediment flux during periods of abrupt warming in the Early Holocene. The association between warming, permafrost thaw, and high erosion-rate and sediment flux is further supported by the landscape response to cooling during the Younger-Dryas, where permafrost recovery and reduced precipitation likely restricted hillslope erosion and sediment transport (Abbott et al., 2000; Mann et al., 2010). Lake sediments from northern Alaska also record an association between charcoal deposition and thermokarst formation, demonstrating the effect of fires on erosion over the last 3 millennia (Chipman & Hu, 2017). In contrast, sediments also record decreased erosion-rate during times of warming. For example, analysis of recent lake deposits in northeast Alaska showed that shrub expansion and lower peak runoff are associated with decreased erosion-rate since 1980, despite increased temperatures (e.g., Tape et al., 2011). Over longer time scales, lake and river deposits in Alaska record a decreased erosion-rate in the Holocene despite increased temperatures, likely reflecting the stabilizing effect of vegetation, peat expansion and decreased aeolian dust supply during this time (Finkenbinder et al., 2015; Gaglioti et al., 2014; Mann et al., 2002). The sedimentary records utilized by these studies appreciably improved the conceptual understanding of this complex system, yet, quantitative estimates of the relative importance of temperature, vegetation, fires, and other key factors remain elusive, as are their functional relationship with erosion-rate and sediment flux.

To explore the association among erosion-rate and various environmental conditions we analyze a data-rich sedimentary record from Burial Lake, northwestern Alaska, that spans glacial-interglacial changes in climate and other environmental conditions and was thoroughly dated and sampled for a broad array of biogeochemical sedimentary proxies for environmental conditions (Abbott et al., 2010; Dorfman et al., 2015; Finkenbinder et al., 2015; Finkenbinder et al., 2018; King et al., 2021; Kurek et al., 2009). This record is used to address the following questions: (a) what sedimentary proxies are most strongly associated with the flux of sediments into the lake (a proxy for erosion-rate), and (b) what are the functional relationship among key sedimentary proxies and sediment flux. Our analysis, based on bi- and multi-variate analyses of the association among sediment flux and biogeochemical sedimentary proxies over the past 25 cal ka BP, quantitatively estimates the relative importance of sedimentary proxies and their relationship with erosion-rate, and in doing so provides insights regarding the dynamics of the arctic system and its potential response to future changes.

## 2. Method

### 2.1. Field Area

Burial Lake (68.43°N, 159.17°W, 460 masl, Figure 1) is located at the northwestern Brooks Range with current mean annual temperature and precipitation of  $-7.5^{\circ}\text{C}$  and 291 mm (King et al., 2021). The lake is approximately circular, with a diameter of  $\sim 1$  km and surface area of  $\sim 0.8$  km<sup>2</sup>. The lake drains a relatively small watershed ( $\sim 3$  km<sup>2</sup>) characterized by moderate to steep slopes ( $1^{\circ}$ – $6^{\circ}$ ) between the lake and surrounding hilltops. Surface runoff into the lake occurs through numerous small gullies with ephemeral streams whose lengths are  $< 1$  km (Figures 1b–1d). The lake's maximal depth is 21.5 m (measured in 2010) and its surface discharge is through a shallow outlet stream with limited flow (Figure 1e), suggesting that the lake is a good sediment trap. The lake watershed is underlain by continuous permafrost with moderate to high ice content and is associated with hillslope thermokarst of moderate to high coverage (Balsler et al., 2016; Olefeldt et al., 2016). The lithology is dominantly composed of moraine deposits that are likely middle Pleistocene or older in age (Hamilton, 2001). The surrounding vegetation is low Arctic tundra dominated by *Salix* spp. *Betula nana*, *Alnus viridis* ssp. *fruticosa*. The lake is oligotrophic and hydrologically open with no evidence of thermal or chemical stratification (Abbott et al., 2010). The lake remained free of glacial influence during the Last Glacial Maximum (26.5–19 ka; Clark et al., 2009), is located just outside the extent of mountain glaciers and Northern Hemisphere ice-sheet (Hamilton, 2001), and contains a relatively long sedimentary record ( $\sim 40$  cal ka BP, Abbott et al., 2010). The lake was cored in the winter of 1998 and in the summers of 1997 and 2010. Two well-dated composite cores (labeled C98 and A10) were used in the analysis presented here. The cores were analyzed for an array of physical, chronological, elemental, and biological measures (Abbott et al., 2010; Dorfman et al., 2015; Finkenbinder et al., 2015; Finkenbinder et al., 2018; King et al., 2021; Kurek et al., 2009).

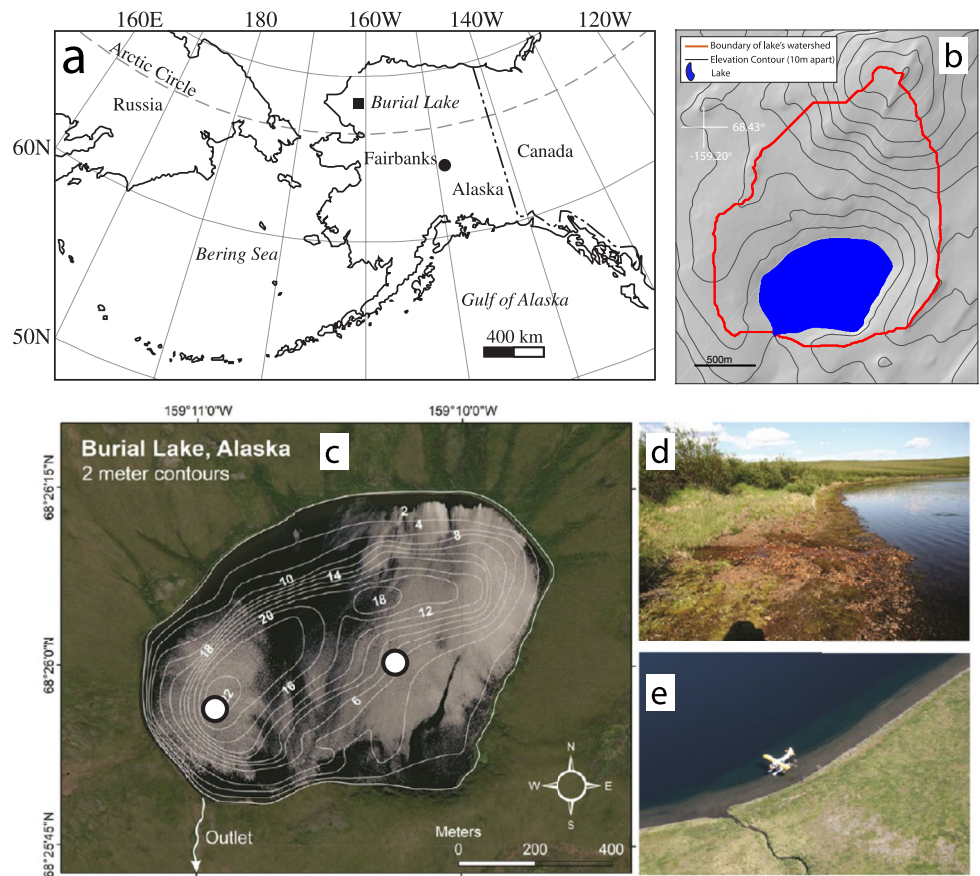


**Figure 1.** Study area (modified from King et al. (2021) and Abbott et al. (2010)). (a) Map showing Alaska and the location of Burial Lake. (b) Hillshade image (based on an IFSAR DEM (Carswell, 2013)) shows the boundary (red line) of the watershed that drains to burial lake. (c) Burial Lake and water depth contours (2 m) on a satellite image (Landers et al., 2008; ArcMap global imagery database). White circles mark the location of cores C98 (right) and A10 (left). (d) Ground view of the eastern of the northern lake shoreline, showing one of the numerous small inlet channels. (e) Aerial view of the outlet channel identified in (c) with floatplane. Photo credits: Mark Abbott, 29 June 2010.

## 2.2. Data Preparation and Types

We use the flux of mineral sediments into the lake (hereafter mineral flux,  $F_d$  [g/cm<sup>2</sup>/yr]) as a proxy for the rate of physical erosion and the resulting sediment flux. Mineral flux (Dorfman et al., 2015) was computed as

$$F_d = \frac{\Delta D}{\Delta t} \rho_d (1 - f_o - f_b). \quad (1)$$

Deposition rate,  $\frac{\Delta D}{\Delta t}$ , is computed from the depths ( $D$  [cm]) of core A10, located close to the depo-center of Burial Lake, and from a <sup>14</sup>C based age model ( $t$  [yr]). Bulk dry density,  $\rho_d$ , the organic matter weight percent (based on loss on ignition at 550°C),  $f_o$ , and biogenic silica weight percent  $f_b$  (Finkenbinder et al., 2015).

The age-model used is based on <sup>14</sup>C measurements collected from multiple studies (Abbott et al., 2010; Dorfman et al., 2015; Finkenbinder et al., 2015; Finkenbinder et al., 2018; King et al., 2021; Kurek et al., 2009) as well 10 new <sup>14</sup>C ages sampled and analyzed for this study. The data collection and processing follows the protocol described in Abbott et al. (2010). The age model for this study is based on 24 radiocarbon dates measured using wood, seeds, and plant macrofossils from A10 and C98 cores. The samples were prepared as described in Finkenbinder et al. (2015), pre-treated using methods described in Abbott and Stafford (1996) and analyzed at the W.M. Keck Carbon Cycle AMS Laboratory, University of California, Irvine. Radiocarbon ages were then calibrated using CALIB 8.2 and the INTCAL20 calibration curve (Reimer et al., 2020). The composite age-depth model

was developed using a Markov chain Monte Carlo statistics-based Bacon approach (Blaauw & Christen, 2011) implemented in R (Blaauw et al., 2021).

Analysis of association between mineral flux and biogeochemical sedimentary proxies relied on data produced through multiple studies of sediment cores from Burial Lake (Abbott et al., 2010; Dorfman et al., 2015; Finkenbinder et al., 2015; Finkenbinder et al., 2018; King et al., 2021; Kurek et al., 2009). We focused on 10 sedimentary proxies (Figure 2) reflecting environmental conditions that might influence erosion-rate: (a) Mean July temperature [ $^{\circ}\text{C}$ ] based on Chironomid assemblage (source: Kurek et al. (2009)); (b) Normalized pollen counts (source: Abbott et al. (2010), labeled pollen sum/exotics in Figures 2–5), computed by normalizing the total count of pollen grains by the count of artificially added exotic pollen grains (used as a counting reference) (Abbott et al., 2010; Salgado-Labouriau & Rull, 1986). Increased pollen count is associated with increased pollen productivity and background pollen flux, and may be indicative of increased vegetation abundance (Qin et al., 2020; Sugita, 2007); (c) Percent pollen from trees and shrubs (PTS, labeled Trees & Shrubs [%] in Figures 2–5) relative to a total of trees, shrubs and herbs (source: datasets associated with Abbott et al. (2010)). Increased PTS may reflect a higher relative abundance of trees and shrubs; (d) Charcoal-based proxy for frequency of local fires [ $\text{ka}^{-1}$ ] (e.g., P. E. Higuera, Chipman, et al., 2011; Chipman & Hu, 2017). The charcoal data was obtained as part of this study, and produced through treatment of contiguous, 1 cc, sediment samples in a solution of sodium hexametaphosphate and bleach for 24 hr. Each sample was then washed through a 125  $\mu\text{m}$  sieve and counted under a stereomicroscope according to the methodology of Whitlock and Larsen (2002). The raw data was processed with the CharAnalysis software (P. Higuera, 2009) with parameters based on values used for lakes in the Noatak Peninsula (P. E. Higuera, Barnes, et al., 2011; P. E. Higuera, Chipman, et al., 2011). Charcoal fragments were collected starting at  $\sim 15$  cal ka BP and older core sections, where charcoal fragments were not found (Vachula et al., 2020), were assigned a zero fire frequency; (e) The ratio of organic carbon to nitrogen ( $C/N$ ) (source: Finkenbinder et al. (2015)). Increased  $C/N$  values are typically associated with increased input of terrestrial compared to aquatic organic matter (Finkenbinder et al., 2015; Meyers & Teranes, 2002), and thus may covary with the magnitude of terrestrial erosion; (f)  $\delta^{18}\text{O}$  [‰] based on Chironomid samples (source: King et al. (2021)). Increased  $\delta^{18}\text{O}$  values can be characteristic of a hydraulic system with a dominant evaporative component that can be associated with a dry climate; (g) Age offset [yr]: the difference between depositional age, as approximated by the age model (i.e., based on macrofossils), and age obtained from bulk sediment samples (source:  $^{14}\text{C}$  ages obtained for this and prior studies). These bulk samples represent an amalgamation of young and aged carbon, sourced from permafrost, active-layer and fresh vegetation from the entire lake watershed as well as from the lake itself (Abbott & Stafford, 1996; Gaglioti et al., 2014; Strunk et al., 2020). Increased age offset likely reflects a higher contribution of old carbon from thawed permafrost, and is therefore expected to covary with erosion and transport of old, permafrost-sourced organic carbon (e.g., Gaglioti et al., 2014); (h) Bulk mean physical grain size [ $\mu\text{m}$ ] (source: Dorfman et al. (2015)). Increased mean grain size is expected to reflect more energetic sediment transport processes (e.g., Macumber et al., 2018), or a decreased flux of aeolian sediments of small grain size (Dorfman et al., 2015; i–j) Ca/K and Ca/Sr ratios, as measured through X-ray Fluorescence (XRF) Spectroscopy (source: Finkenbinder et al. (2015)). Increased ratios can be associated with thermokarst-related mass wasting deposits (Chipman & Hu, 2017). For robustness, we have also run the analysis based on the log of these ratios (Weltje & Tjallingii, 2008). The sedimentary proxies were measured from core A10, with the exception of pollen and Chironomid based data which were measured from core C98. Age offset is based on  $^{14}\text{C}$  samples from both cores.

### 2.3. Data Analysis

#### 2.3.1. Pre-Processing

The different sedimentary proxies were pre-processed to facilitate a robust analysis of their association with mineral flux. Given that different sedimentary proxies were sampled at different depth and age intervals, all proxies were linearly interpolated (e.g., Chipman & Hu, 2017) to age intervals of 100 years (approximately the 25 percentile of sampling age intervals for different sedimentary proxies) between 2 and 25 cal ka BP. Data from  $<2$  cal ka BP were excluded to avoid extrapolation beyond the youngest data points for some of the proxies (pollen, age offset, grain size). Data from  $>25$  cal ka BP were excluded because of a deviation in age-depth relations between cores A10 and C98 that reflects an unconformity in core C98 (Abbott et al., 2010;

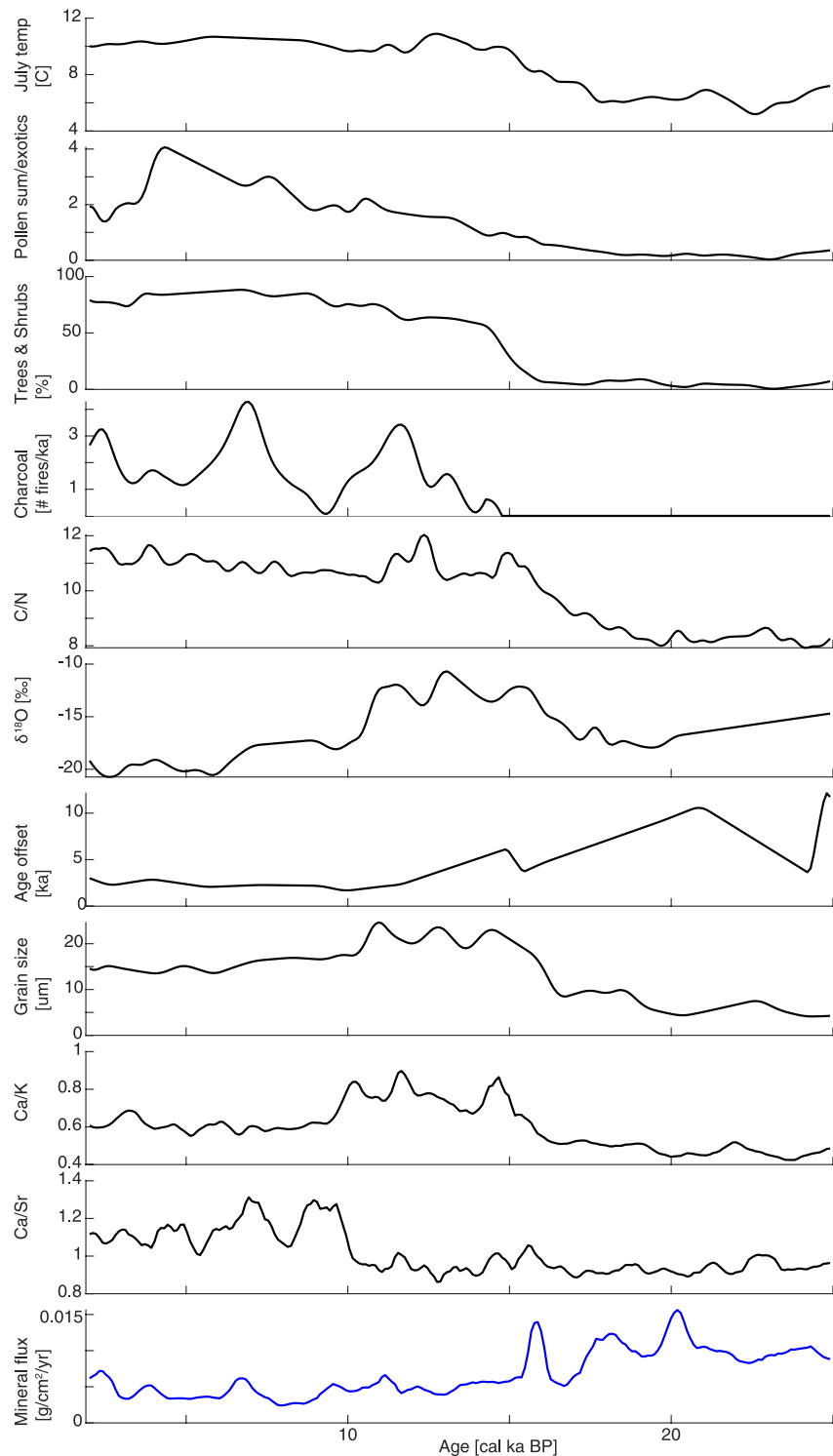


**Figure 2.** Sedimentary proxies. Time series of the proxies described in Section 2.2. Mineral flux, which is used as the response variable in the following analyses, is colored in blue.

Finkenbinder et al., 2015). To acknowledge the age uncertainty associated with individual data points and the associated mismatch between cores, the data was smoothed with a running average filter, whose size (500 years) is defined based on the maximal range of  $^{14}\text{C}$  age uncertainty. The mineral flux ( $F_d$ ) was computed from the interpolated and smoothed age, LOI, and biogenic silica data (Equation 1). This procedure produced a data set of 229

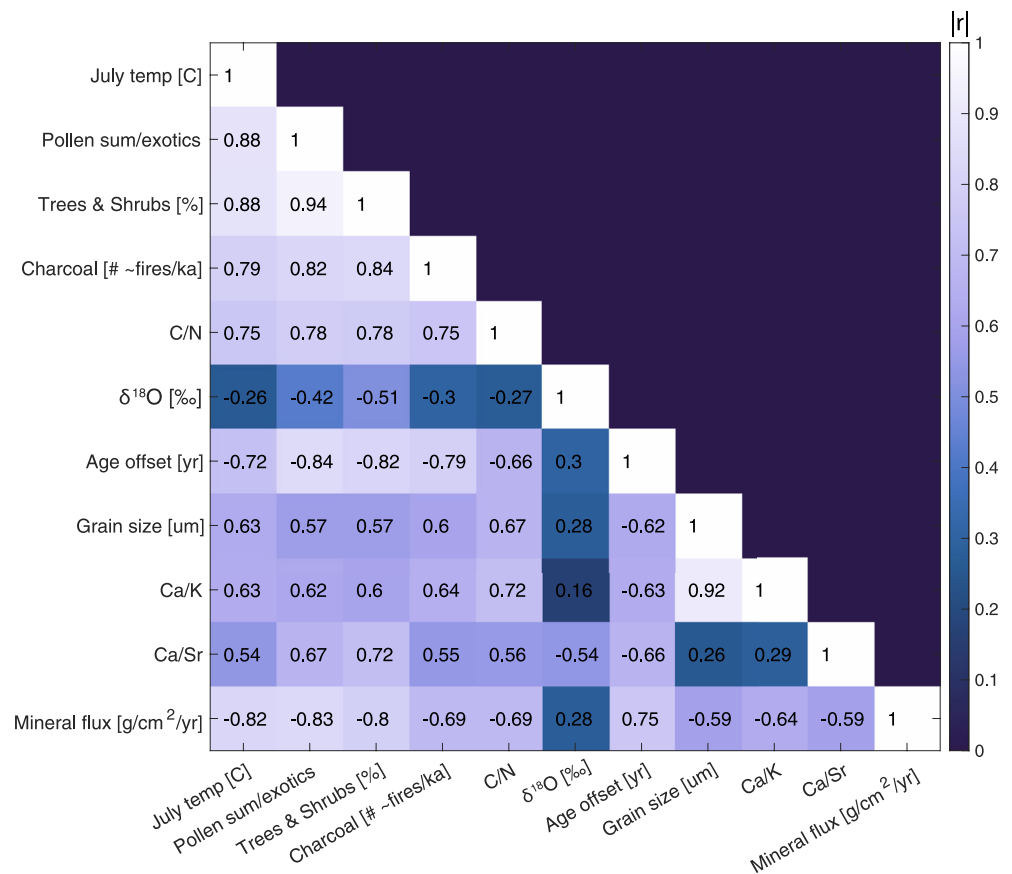


**Figure 3.** Correlation between sedimentary proxies. A heat map of a correlation matrix (Pearson's  $r$ ) for all pairs of sedimentary proxies. To highlight correlated proxies, the map is colored by the absolute value of Pearson's  $r$  ( $|r|$ ), and the displayed text values reflect whether the correlation is negative or positive. All the correlations are statistically significant (significance level  $\alpha = 0.01$ ). The bottom row shows the  $r$  values for correlations between mineral flux and each of the sedimentary proxies.

observations (i.e., an observation for each 100 years time interval), where each observation contains 11 numeric values: a value for each of the 10 sedimentary proxies and for mineral flux (Figure 2).

### 2.3.2. Statistical Analysis

For robustness, we used linear and non-linear bi and multi variate methods to evaluate and rank the strength of association between sedimentary proxies (predictors) and mineral flux (response). The methods include (a) Linear bivariate analysis based on Pearson's correlation coefficient and the associated  $R^2$ . (b) Non-linear bivariate analysis of predictor importance based on random forest (Nicodemus et al., 2010; Wijeyakulasuriya et al., 2020), (c) Linear multivariate analysis of variable importance based on partial least squares regression (e.g., Bodmer et al., 2020; Mehmood et al., 2012), (d) Non-linear multivariate analysis based on a random forest model (Breiman, 2001; Kursu & Rudnicki, 2010). Below we briefly describe these methods (a more detailed description of the methods and their associated parameters is available in Supporting Information S1).

### 2.3.3. Random Forest

To quantify the association between sedimentary proxies (predictors) and mineral flux (response) while accounting for complex non-linear relationships we used random forest based analyses. Random forest (Breiman, 2001) is an ensemble of binary regression trees, each recursively grown (hereafter trained) with a random subset of the observations (i.e., in bag observations). At each split in the tree, a random subset of predictors is selected to be available for splitting, and a split is made based on the predictor that best split the response variable into more homogenous groups. The predictive power of the trained trees can then be evaluated based on the observations that were not used in the training (i.e., out of bag observations). Random forest models are advantageous in that

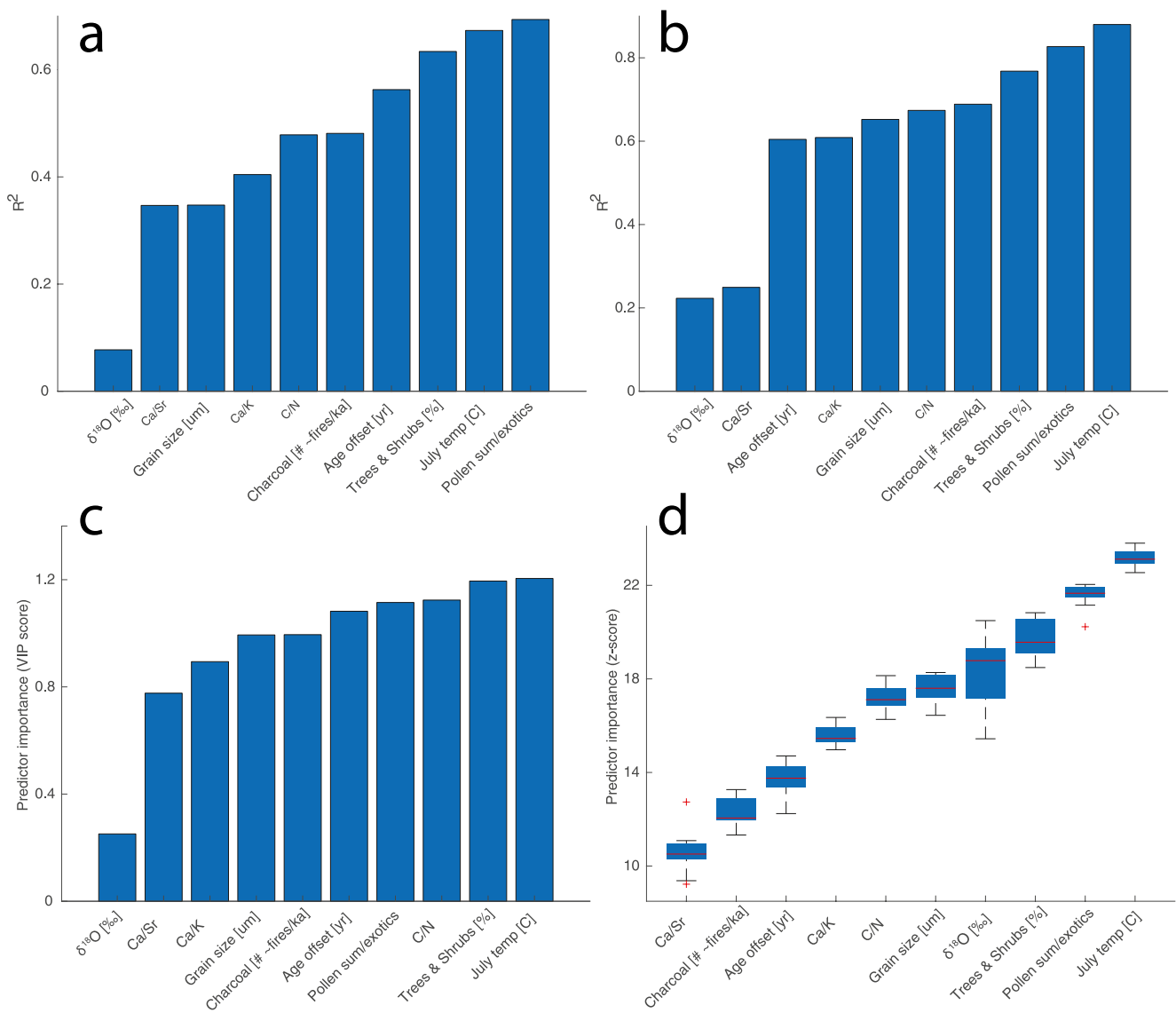


**Figure 4.** Predictor importance. Bar and box plots showing a relative ranking of sedimentary proxies based on the strength of association between mineral flux (a proxy for the rate of physical erosion) and different sedimentary proxies. The top panels (a and b) show rankings based on bivariate analyses and the bottom panels (c and d) show rankings based on multi-variate analyses. The left column of panels (a and c) show analyses that assume linear association and the right column (b and d) show analyses that are not restricted by this assumption. (a)  $R^2$  values based on Pearson's  $r$ , (b)  $R^2$  values based on random forest, (c) Variable importance in projection (VIP) based on partial least squares regression, (d) Z-score values based on Boruta analysis that employs an iterative random forest procedure. The red line marks median, whiskers extend to 1.5 times the interquartile range, and “+” symbols mark outliers.

they do not make assumptions about data distribution and the form of the relations between the predictors and response variable and their prediction is mostly insensitive to correlated predictors (e.g., Aliyuda et al., 2020; Konapala & Mishra, 2020; Vaughan et al., 2017). Random forest models are particularly suitable for analysis of complex natural systems that are influenced by multiple factors (e.g., Aliyuda et al., 2020; Cotton et al., 2016; Konapala & Mishra, 2020; Rafat et al., 2021; Vaughan et al., 2017) (a more detailed description of random forest is available in Supporting Information S1).

### 2.3.4. Predictor Importance

We used the Boruta procedure (Kursa, 2014; Kursa & Rudnicki, 2010), based on a multivariate random forest model, to identify predictors (sedimentary proxies) whose association with the response variable (mineral flux) is statistically significant and to rank their importance (computed via a z-score metric) while accounting for potential interactions between predictors. For a comprehensive assessment of importance, we also used random



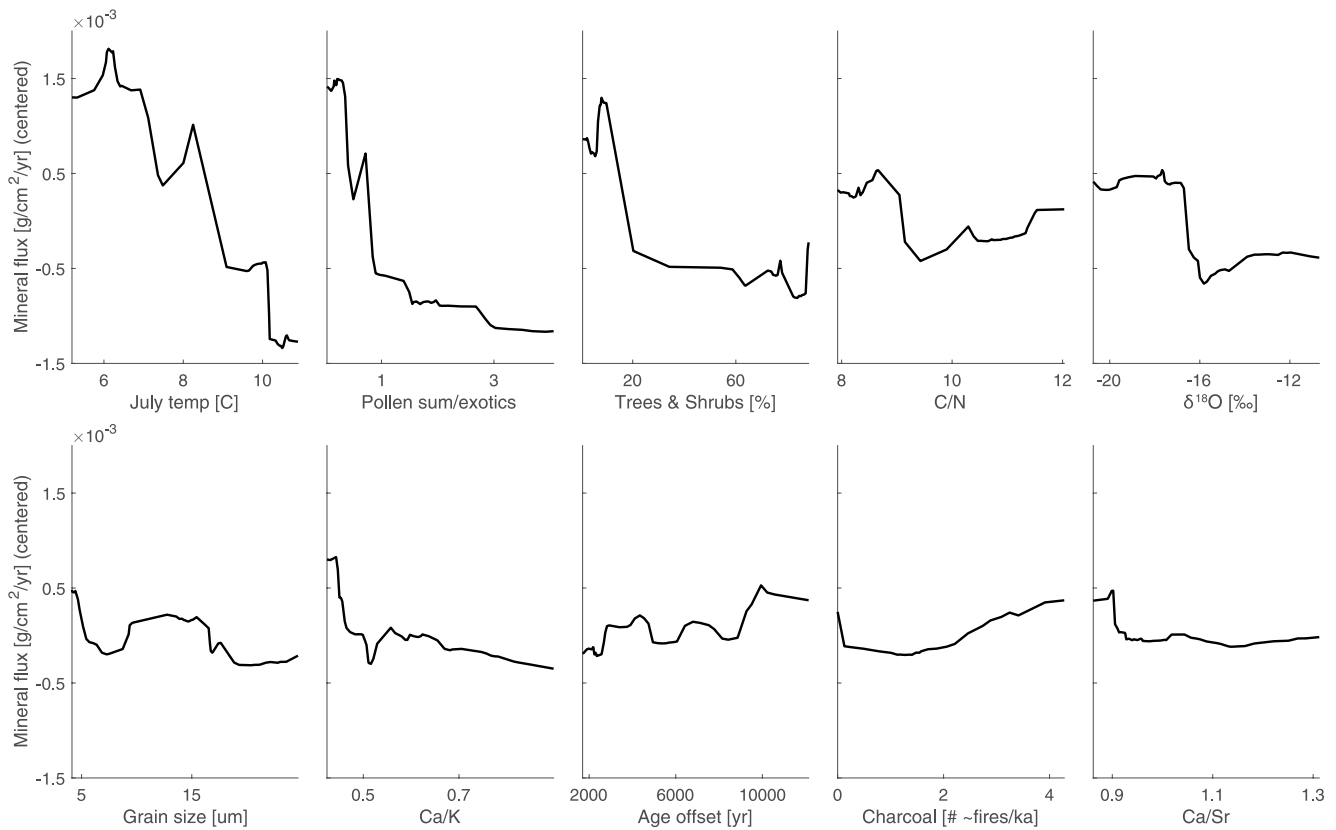


**Figure 5.** Accumulated local effects (ALE) plots. ALE plots, based on a random forest model, display the marginal dependence of mineral flux on different sedimentary proxies. The  $x$ -axis shows the values of each sedimentary proxy, and the  $y$ -axis shows mineral flux values centered by the mean mineral flux for each plot (i.e., negative values reflect fluxes that are lower than this mean). All plots have the similar  $y$ -axis scaling, and thus changes in the amplitude of the plots reflect differences in the marginal effect of different proxies.

forest models to quantify the bivariate association between mineral flux to each sedimentary proxy separately (computed via an  $R^2$  metric) (Nicodemus et al., 2010; Wijeyakulasuriya et al., 2020).

For robustness in predictor importance estimates, we also used linear multi and bi variate analyses to rank predictor importance. We ranked the importance of the predictors (sedimentary proxies) through a variable importance in projection (VIP) predictor ranking based on multivariate partial least squares (PLS) regression (e.g., Bodmer et al., 2020; Mehmood et al., 2012). PLS combines the advantages of multiple linear regression and principal component analysis by finding orthogonal combinations (components) of the original predictors that have a large covariance with the response variable. The orthogonality of these components resolves multicollinearity issues, and their covariance with the response variable produces a reliable predictive power (e.g., Kemsley, 1996; Mehmood et al., 2012) while accounting for potential associations between predictors. For robustness, we also evaluated the strength of bivariate linear association between each predictor and the response (mineral flux) using Pearson's correlation coefficient ( $r$ ) and the associated  $R^2$ .

### 2.3.5. Relationships Between Key Sedimentary Proxies and Mineral Flux

To explore the relationships between key sedimentary proxies and mineral flux, while accounting for potential non-linearities as well as for correlated predictors, we use accumulated local effect (ALE, Apley and Zhu, 2020) based on a multivariate random forest model (Friedman, 2001). ALE is a relatively new method for analysis and visualization (Galkin et al., 2018; Stein et al., 2021; Xenochristou et al., 2021) that is advantageous over a standard partial dependence analysis (i.e., Friedman, 2001; Konapala & Mishra, 2020; Vaughan et al., 2017) in that it helps interpret the marginal effect of correlated predictors by eliminating improbable combinations of such predictors.

The Boruta and ALE analyses were executed with the R packages “Boruta” (Kursa & Rudnicki, 2010) and “iml” (Molnar, 2018). All other analyses were conducted with MATLAB (MATLAB, 2021).

### 3. Results

The statistical models we used explain most of the variance in the erosion-rate data (i.e., high predictive power), and sedimentary proxies are often correlated (Figures 3 and 4). Multivariate random forest and PLS analyses produced  $R^2$  values of  $\sim 0.93$  and  $0.79$ , respectively. Bivariate analyses produced varying  $R^2$  values for different parameters, with highly ranked sedimentary proxies having  $R^2$  values  $>0.8$  and  $>0.7$  for the bivariate random forest model and Pearson's correlation, respectively (Figures 4a and 4b). The absolute value of Pearson's correlation ( $r$ ) between sedimentary proxies is often high and can exceed  $0.9$  (Figure 3) and the correlation is statistically significant for all proxies (significance level  $\alpha = 0.01$ ).

Different methods for ranking of predictor importance reveal both consistencies and differences in predictor ranking (Figure 4). The Random Forest based Boruta procedure (Figure 4d), the least restrictive of the methods, identified all 10 predictors (sedimentary proxies) as statistically important (i.e., see Supporting Information S1 for details), and ranks July temperature, percent pollen from trees and shrubs (PTS), and normalized pollen counts as the most important proxies. These sedimentary proxies are ranked within the top four predictors by all other methods (Figures 4a–4c). The sedimentary proxies C/N, grain size, and  $\delta^{18}\text{O}$  are ranked as having a medium relative importance by the Boruta procedure, and as having either high or low importance by the other methods. The sedimentary proxies Ca/Sr, Ca/K (or the log of these ratios, Supporting Information S1), charcoal-based fire frequency, and age offset, are ranked low by the Boruta procedure, and have either medium or low importance according to other methods.

The trend of the relations between mineral flux and key sedimentary proxies (Figure 2) is generally consistent between ALE (Figure 5) and bivariate correlation (Figure 3). Mineral flux generally increases with increased Age offset, and decreases with increased July temperature, PTS, normalized pollen counts, grain size, C/N, and Ca/K. The trend of relations between mineral flux and the proxies  $\delta^{18}\text{O}$ , and charcoal-based fire frequency are inconsistent between ALE and bivariate correlation. Overall we consider the random-forest based ALE analysis more robust as it account for interactions with other proxies and is not restricted by an assumption of linearity.

Although most ALE relations are somewhat noisy, they typically display a clear positive or negative association with mineral flux (Figure 5). Increased mean July temperature from  $\sim 5^\circ\text{C}$  to  $11^\circ\text{C}$ , for example, is associated with a decreased mineral flux of approximately  $0.003 \text{ g/cm}^2/\text{yr}$ , which is  $\sim 44\%$  of the mean mineral flux into the lake between 25 and 2 cal ka BP ( $0.0068 \text{ g/cm}^2/\text{yr}$ ). For some proxies, the ALE relation show a step like dependency between mineral flux and sedimentary proxies. For example, a step like decrease in mineral flux of approximately  $0.0023 \text{ g/cm}^2/\text{yr}$  ( $\sim 34\%$  of the mean mineral flux over the analyzed period) occurs when the normalized pollen counts (labeled pollen sum/exotics in Figures 2–5) exceed a value of  $\sim 1$ . A similar drop in mineral flux occurs when the PTS (labeled trees & shrubs [%] in Figures 2–5) exceeds a threshold of  $\sim 20\%$ . Step like drops in mineral flux of various magnitudes ( $\sim 0.00015$ – $0.0005 \text{ g/cm}^2/\text{yr}$ ) also occur with increased C/N,  $\delta^{18}\text{O}$ , Ca/Sr, and Ca/K. Likewise, the mineral flux abruptly drops by  $0.0005 \text{ g/cm}^2/\text{yr}$  ( $\sim 7\%$  of the mean mineral flux over the analyzed period) when the mean grain size exceeds a threshold of  $\sim 6 \mu\text{m}$ , a drop which is followed by non-monotonic changes in mineral flux. A gradual increase in mineral flux of approximately  $0.0006 \text{ g/cm}^2/\text{yr}$  ( $\sim 9\%$  of the mean mineral flux over the analyzed period) occurs when the charcoal-based fire frequency exceeds a threshold of 1.5 fires per ka. A similar increase in mineral flux, albeit noisy, is associated with increased age offset from 2 to 11 ka.

## 4. Discussion

### 4.1. Associations Between Key Sedimentary Proxies and Mineral Flux

The random forest based Boruta procedure (Kursa, 2014; Kursa & Rudnicki, 2010, Figure 4d) identified all 10 predictors (i.e., sedimentary proxies) as statistically important (Supporting Information S1). Assuming that mineral flux represents the magnitude of physical erosion over the lake watershed, and that the associations we analyzed reflect causative relations, this suggests that all the sedimentary proxies we analyzed influence erosion-rate in a meaningful way. Although all proxies are statistically important, some are more important than

others, as reflected by the  $> \times 2$  difference in the measures of importance between ranked proxies (Figure 4). The ranking of sedimentary proxies (Figure 4), also reflected in the relative amplitude of the ALE plots (Figure 5), suggests that temperature, normalized pollen counts, and PTS, have a dominant effect on erosion-rates. Proxies related to terrestrial versus aquatic productivity (C/N) and sediment transport mechanisms (mean grain size) are ranked as having medium importance, and proxies related to erosion of old carbon (age offset), watershed and regional hydrology ( $\delta^{18}\text{O}$ ), mass wasting (Ca/K, Ca/Sr) and charcoal-based fire frequency are ranked as having medium to low importance. Whereas all these proxies are statistically important, this ranking highlights the importance of temperature and vegetation in controlling erosion-rates in the Burial Lake watershed over the analyzed period. To the extent of our knowledge, this is the first study that systematically quantifies and ranks the effect of multiple proxies on erosion-rate in permafrost areas. Therefore we are unable to quantitatively compare the patterns we observe to other studies. Nevertheless, we are able to compare our results on the general direction and drivers of erosion-rates with other periglacial watersheds described in the literature.

The negative association between mineral flux and mean July temperature (Figures 3 and 5) may appear counterintuitive. Temperature is ranked as a highly important predictor by all methods (Figure 4) and the ALE plots (Figure 5) suggest that a temperature increase of  $\sim 6^\circ\text{C}$  is associated with a  $\sim 44\%$  decrease in mineral flux (relative to the mean mineral flux:  $0.0068 \text{ g/cm}^2/\text{yr}$ ). Increased temperatures are often expected to increase erosion-rates through thermokarst expansion, thus producing a positive, rather than negative association between mineral flux and temperatures (e.g., Gooseff et al., 2009; Kokelj & Jorgenson, 2013; Lafrenière & Lamoureux, 2019; Lantz & Kokelj, 2008; Lewkowitz & Harris, 2005; Mann et al., 2002; Mann et al., 2010). For example, in the north slope of Alaska, episodes of increased temperatures (14–12.8 and 11.5–9.5 cal ka BP) during the Pleistocene-Holocene transition were associated with increased flux of sediments to floodplains, likely the outcome of widespread mass wasting associated with permafrost thaw (Mann et al., 2010). In light of such findings, the negative association between temperature and mineral flux (Figures 3 and 5) suggests that in Burial Lake thaw related mass wasting processes are negligible compared to other sediment transport processes. This is supported by the relative minor association between mineral flux and Ca/K or Ca/Sr (Figure 4), which were used as proxies for sediments delivered to lakes by thermokarst mass wasting processes (i.e., Chipman & Hu, 2017), as well as by the negative, rather than positive, association between mineral flux and these proxies (Figures 3 and 5). Although this may indicate that mass wasting processes next to Burial Lake have different elemental characteristics compared to those studied by Chipman and Hu (2017), the lack of large topographic scarps produced by past mass wasting processes in the watershed of Burial Lake (Figure 1) further corroborates the relatively minor role of such processes in this basin.

Various processes may explain a negative association between temperature and mineral flux. For example, (a) Increased temperature and moisture can enhance paludification and expansion of vegetation that stabilize the landscape and protect it from erosion (e.g., Gaglioti et al., 2014; Mann et al., 2002; Mann et al., 2010), and also insulate the underlying soil from the warming atmosphere (Baughman et al., 2015; Mann et al., 2002), potentially inhibiting thaw and thermokarst; (b) Warming induced thickening of the active layer may increase the magnitude of subsurface flows (S. Lamoureux, 2000; O'Connor et al., 2019; Woo, 1983) at the expense of erosive surface flows; (c) Warm spring seasons may decrease the flashiness of spring floods and the erosion they cause (Cockburn & Lamoureux, 2008a; Woo & Sauriol, 1980); and (d) Warming related changes in wind patterns and in availability of allochthonous sediment sources that can reduce aeolian supply of mineral material (Dorfman et al., 2015) as well as shoreline erosion. Although the specific mechanisms through which increased temperature causes decreased erosion-rate remain uncertain, our findings highlight the potential importance of such response.

Normalized pollen counts and PTS are ranked as highly important proxies by all methods (Figure 4). An increase in the value of these proxies is associated with step-like decrease of about 30% (relative to the mean mineral flux) in mineral flux (Figure 5). This negative association provides hints about the processes through which vegetation influences erosion in the watershed of Burial Lake. Increased pollen counts may reflect increased abundance of vegetation in the region, as well as increased pollen productivity and/or background pollen deposition (Qin et al., 2020; Sugita, 2007). Assuming that mineral flux represents the intensity of physical erosion over the lake watershed, the negative association between mineral flux and normalized pollen counts (Figures 3 and 5) likely reflects decreased erosion-rate with increased vegetation abundance. Such increased abundance can cause expansion of root systems that reinforce the soil and decrease its erodibility, as well as increased density of leaves and branches that can trap sediments delivered from upslope and intercept rain drops whose impact can

cause erosion (Gyssels et al., 2005; S. Lamoureux, 2000; Tape et al., 2011). Further, soil cover by vegetation, interlocked roots, and dead plant matter can help insulate the soil from temperature fluctuations, reducing supply of erodible mineral matter to the surface via frost-heave processes (Mann et al., 2002). The development of a permeable organic horizon in periods of increased vegetation cover and peat development (Evans et al., 2020; Mann et al., 2002; O'Connor et al., 2019) can help transmit water through subsurface rather than surface flows (Lamoureux, 2000; O'Connor et al., 2019; Woo, 1983). This can decrease the magnitude of erosive surface flows and their sediment transport capacity. The effect of vegetation on erosion-rate is also reflected by the negative association between mineral flux and the PTS (Figures 3 and 5). This suggests that around Burial Lake, shrubs and trees primarily stabilize permafrost soils (Nauta et al., 2014; Tape et al., 2011), rather than destabilizing them through winter insulation, increased soil temperature, and protrusion through snow that enhance permafrost thaw (Bonfils et al., 2012; Kropp et al., 2020; Wilcox et al., 2019). The threshold decrease in mineral flux with increased normalized pollen counts and PTS (Figure 5) is consistent with geomorphic theory and findings (Cerda, 1999; Schumm, 1979; Sun et al., 2019), and likely reflects a non-linear effect of vegetation and shrub expansion on the connectivity of fluvial and sediment transport processes. The effect of vegetation on erosion may also be reflected in the somewhat high ranking of C/N (Figure 4) and its overall negative association with mineral flux (Figures 3 and 5). High C/N values are typically indicative of high contribution of terrestrial plant matter from the lake watershed relative to aquatic organic matter formed in the lake (Finkenbinder et al., 2015), and may reflect increased vegetation cover in the watershed and its transport to the lake. Overall, our findings suggest that increased vegetation abundance, as well as increased relative abundance of shrubs and trees, meaningfully reduced the erosion of mineral matter in the watershed of Burial Lake.

The negative association between  $\delta^{18}\text{O}$  and mineral flux (Figure 5) is consistent with intuitive expectations. An increase in the value of  $\delta^{18}\text{O}$  above  $-16\text{‰}$  is associated with a step-like decrease of about 16% (relative to the mean mineral flux) in mineral flux (Figure 5). Increased  $\delta^{18}\text{O}$  values can be characteristic of a hydrologic system with a strong evaporative component, a condition that may prevail in dry periods when precipitation is low (King et al., 2021). Low precipitation is likely associated with reduced fluvial erosion and increased slope stability, resulting in decreased mineral flux with increased  $\delta^{18}\text{O}$  (Figure 5). Evaporative conditions may also be associated with low lake levels in Burial lake (King et al., 2021) when reworking of lake sediments through lake shore erosion may take place (Gaglioti et al., 2014), yet the negative association between  $\delta^{18}\text{O}$  and mineral flux suggests that if this process occurs in Burial Lake it has a relatively minor contribution to the mineral flux measured near the lake's depo-center where core A10 was collected. The shift in the ranking of  $\delta^{18}\text{O}$  between the Boruta procedure (Figure 4d) and the other procedures (Figures 4a–4c), may reflect a sensitivity of ranking methods based on permutation-importance to correlated predictors (Hooker et al., 2021). The overall medium-low ranking of the  $\delta^{18}\text{O}$  predictor as well as the non-linear association between  $\delta^{18}\text{O}$  and mineral flux, hints that the proposed mechanistic view of the association between  $\delta^{18}\text{O}$  and mineral flux may be somewhat simplistic and does not capture the true hydrologic complexity of the lake system. For example,  $\delta^{18}\text{O}$  in sediments does not depend only on precipitation-evaporation balance, as it is also sensitive to the  $\delta^{18}\text{O}$  of the source water (precipitation and ground water), whether the lake is well mixed or not, and the effect of wind intensity on evaporation (Braig et al., 2010; King et al., 2021).

Age offset, the difference between bulk  $^{14}\text{C}$  ages and the macrofossil-based depositional age, is positively correlated with mineral flux (Figures 3 and 5), which is generally consistent with expectations. An increase in the value of age offset from 2 to 11 ka is associated with about 10% increase in mineral flux (relative to the mean mineral flux, Figure 5). Large age offsets likely represent increased contribution of old carbon, derived from organic matter stored in permafrost (Abbott & Stafford, 1996; Gaglioti et al., 2014; Strunk et al., 2020). Given that the age of permafrost sourced carbon increases with soil depth due to deposition and paludification (Murton et al., 2015; Palmtag et al., 2015; Shelef et al., 2017), periods of increased age offset can be interpreted as being associated with deep incision that erodes and transports old carbon from deep soil horizons (Gaglioti et al., 2014; Vonk et al., 2012). Alternatively, high age offset may reflect a steep age-depth gradient in permafrost soils, such that even shallow incision can erode and transport old carbon into the lake. In Burial Lake, high age offset occurs primarily before the expansion of vegetation based on the trend of normalized pollen count (Figure 2), and is likely associated with times of poorly developed soil organic layer and steep age-depth gradient in soils across the watershed. The negative association between age offset and grain size ( $r = -0.62$ , Figure 3) may support this interpretation, as deep fluvial incision coincides with deep and fast flows that can transport large grains (e.g., Golden & Springer, 2006; Kociuba & Janicki, 2015), resulting in positive, rather than negative association

between age offset and grain size. This suggests that the positive correlation between mineral flux and age offset reflects the transport of old carbon through shallow erosional processes that delivered a relatively large quantity of fine sediments to the lake.

The non-linear relation between mineral flux and mean bulk grain size (Figure 5) may point at key processes of sediment transport. The step like increase in mineral flux (8% relative to the mean mineral flux) at grain sizes smaller than  $\sim 6 \mu\text{m}$  (Figure 5), likely reflects the important contribution of mineral matter transported via aeolian process (Dorfman et al., 2015). Once deposited in the lake's watershed, this small grain size fraction can be transported into the lake by fluvial flows of low magnitude, resulting in a high mineral flux that is somewhat independent of the magnitude of incision and fluvial flows across the watershed. This is consistent with the association between age offset, mineral flux and grain size described above. The non-monotonic relation between mineral flux and grain size at size fractions larger than  $\sim 6 \mu\text{m}$  is consistent with a proposed decoupling between grain size and mineral flux in Arctic lakes (Cockburn & Lamoureux, 2008b).

Fires are expected to increase erosion-rate and mineral flux as they are associated with permafrost degradation, thermokarst, and removal of vegetation (Chipman & Hu, 2017; B. M. Jones et al., 2015; Patton et al., 2019). This is generally consistent with the increased mineral flux (9% relative to the mean mineral flux) when charcoal-based fire frequency estimates exceed 1.5 fires per ka (Figure 5). However, the expected relation between fire frequency and mineral flux contrasts with an exceptionally high mineral flux at a period of very low fire frequency prior to 15 cal ka BP (Figure 2), when vegetation was potentially too sparse to sustain an active fire regime. This may reflect the aforementioned high aeolian sourced mineral flux in this period (Dorfman et al., 2015; Finkenbinder et al., 2015). The relative low importance of charcoal-based fire frequency (Figure 4) suggest that in Burial Lake, the contribution of fires to erosion-rate is small compared to that of other proxies, which is consistent with the low ranking of proxies related to mass wasting, a process that can be triggered by wildfires (Chipman & Hu, 2017).

#### 4.2. Temporal Context

Viewed in a temporal context, changes in mineral flux in Burial Lake can be coarsely divided to two periods (Figure 2). A period of high mineral flux between 25 and  $\sim 16$  cal ka BP, which is primarily associated with high values of age offset, and low values of mean July temperature, normalized pollen counts, PTS, charcoal-based fire frequency, C/N and grain size. This period coarsely overlaps with the last glacial maximum, and was dominated by cold, dry and windy climate, low lake levels, and low sea level that exposed the Beringian continental shelves, a potential source for aeolian dust for Burial Lake (Dorfman et al., 2015; Finkenbinder et al., 2015; King et al., 2021). These conditions are conducive for high aeolian flux of small grain size detritus, low vegetation productivity (i.e., resulting in low fire frequency and low C/N), and poorly developed soil organic layer that facilitates high age offset even when incision is shallow. The low lake levels may have contributed to increased erosion-rate by increasing the topographic slope adjacent to the lake during this period, as well as by reworking of old deposits that contributed to the increased age-offset (e.g., Gaglioti et al., 2014). The following period, from  $\sim 16$  to 2 cal ka BP, is characterized by an overall decrease in mineral flux, which is associated with a decrease in age offset, and an increase in temperature, normalized pollen counts, PTS, fire frequency, C/N and grain size. This period coarsely aligns with the Late Glacial-Holocene transition (including the Bølling-Allerød (15–12.9 ka) and Younger Dryas [12.9–11 ka]) and extends to the Holocene. It is generally associated with warmer, wetter and less windy conditions compared to the prior period (with potential exceptions during the Younger Dryas), accompanied by rising lake and sea levels, increased vegetation productivity and peatland development (Dorfman et al., 2015; Finkenbinder et al., 2015; Jones & Yu, 2010; King et al., 2021; Mann et al., 2002). These changes can cause the decreased flux of fine aeolian detritus and the associated increase in mean grain size. The decrease in mineral flux at this period, despite evidence for increased precipitation, likely reflects the stabilizing effect of peat and shrubs (Gaglioti et al., 2014; Nauta et al., 2014; Tape et al., 2011) that protected the landscape from physical erosion and insulated it thermally, thus inhibiting erosion and permafrost thaw in spite of increased temperatures and precipitation. The decreased erosion and increased paludification likely decreased the delivery of old carbon to the lake, as reflected by decreased age offset. Although periods of rising lake level can cause thermokarst expansion and lake shore erosion (Gaglioti et al., 2014), the relatively low mineral flux and decreased age offset over this period suggest that this is not a meaningful process in Burial Lake. This is consistent with the findings of Gaglioti et al. (2014), showing that most of the old carbon in lake deposits (i.e., Lake of the Pleistocene/Nikivlik lake, located  $\sim 120$  km east of Burial Lake) is sourced from the watershed and not from lakeshore erosion.

### 4.3. Limitations and Future Research Directions

Our analyses and interpretation are underlain by some key assumptions. The interpretation, like most limnology based paleo-climate studies, implicitly assumes that sediments are deposited in the lake soon after they are eroded (i.e., within the uncertainty in deposits age) without shredding the environmental signal (e.g., Jerolmack & Paola, 2010), so that the sedimentary proxies reflects the condition in the watershed at the time of deposition. This assumption is likely valid given the small scale of the analyzed watershed, and the relative quiescence of the lake. We also assume that the Sadler effect (i.e., Sadler, 1981) is negligible based the continuous sedimentation recorded by the cores, and the lack of indicators for mechanisms that may cause hiatuses (e.g., no accommodation space, diversion of channel systems) (Jenny et al., 2019). Further, our interpretation sometimes assumes causative relations between sedimentary proxies for environmental conditions and erosion-rate, while the analysis itself reflects association, not causation. Whereas time lagged analysis may help identify causative relations (e.g., Granger, 1969), it is possible that clear unidirectional causative relations do not exist in this system, as it may be characterized by feedbacks between its components (e.g., between erosion, vegetation and hydrology).

Although our findings provide insights regarding the first order association between mineral flux and environmental conditions, they are based on a single (albeit data rich) field area and refer to a limited set of processes. For example, we focused on physical erosion and particulate deposits, and did not address the role and magnitude of chemical erosion which can be an important process in Arctic and/or carbonate watersheds (Anderson & Anderson, 2010; Huh & Edmond, 1999; Ryb et al., 2014). Similarly, the analyzed watershed is relatively small with surrounding hill slopes drained by zero to first order channels (Figure 1). While such small watersheds and hill-slopes occupy most of the global landscape (e.g., Horton, 1945; Pelletier et al., 2016) and are key in understanding and quantifying erosional processes, their analysis does not capture processes such as incision and bank erosion by large rivers (Costard et al., 2007; Payne et al., 2018). Likewise, the association between erosion-rate and lake level changes is not directly addressed in our analysis because of the high uncertainty in paleo lake levels and the small number of temporal constraints on lake-level compared to other predictors (Finkenbinder et al., 2015). Additionally, the long sedimentary record in Burial Lake captures periods of large changes in environmental conditions and their influence on erosion-rate (e.g., late glacial to early Holocene transition). However, the influence of such periods on the predictors-response associations may mask patterns that occur over relatively stable period such as the Holocene (Finkenbinder et al., 2015; Kurek et al., 2009). Separate analysis of periods of relative stability may reveal hidden patterns with additional implications for a warmer Arctic. Finally, the analysis is based on the sedimentary record of a single lake, and although the associations we quantify are similar to those suggested in other sites in northern Alaska (Gaglioti et al., 2014; Tape et al., 2011), it is not clear over what temporal and spatial scales these associations can be extrapolated. Robust analyses of multiple lakes across the Arctic can help address these knowledge gap.

### 4.4. Implications

Increased warming, precipitation, shrub expansion and fire frequency are predicted in the coming century (Bintanja & Andry, 2017; Heijmans et al., 2022; McCarty et al., 2021; Meredith et al., 2019) and can affect erosion and sediment transport across the Arctic, which may in turn influence thaw, carbon emissions and delivery of sediments and carbon to the aquatic system. However, the direction and magnitude of future changes in erosion is challenging to predict. Our analysis suggests that increased temperature and shrub expansion will be associated with decreased erosion-rate in areas akin to the Burial Lake watershed (Figures 4 and 5). Whereas this decreased erosion-rate may be counteracted by the effects of increased fire frequency and thermokarst (the study area is associated with hillslope thermokarst of moderate to high coverage (Olefeldt et al., 2016)), the relatively low ranking and marginal effect of charcoal-based fire frequency, as well as of the Ca/Sr and Ca/K ratios (Figures 4 and 5), hints that the influence of these processes on catchment wide erosion-rate in areas akin to the Burial Lake watershed may be low. Such predictions, however, should be taken with caution, as future environmental conditions may differ from past ones in terms of predictor values and combinations, so that paleo-information from the sedimentary record may not be directly applicable for predictions. For example, the temporal contextualization in Section 4.2 suggests that decreased erosion-rate is associated with the development of peat (Jones & Yu, 2010; Mann et al., 2002), which may not have a direct future analogue. Despite these limitations, some of the first order patterns we observe can likely guide future predictions. For example, the dominant and negative associations between mineral flux and proxies related to vegetation abundance and shrubs expansion point at the primary

importance of vegetation in regulating erosional processes in Arctic settings. Similarly, the threshold response of erosion-rate to vegetation-related proxies, as well as to  $\delta^{18}\text{O}$ , C/N, and charcoal-based fire frequency, highlight the potential for strong non-linear changes in erosion in response to future changes in Arctic conditions.

## 5. Summary

This study explores the association between erosion and environmental changes in permafrost covered landscapes. It relies on a data-rich sedimentary record from Burial Lake, Alaska, to decipher the complex interaction among erosion-rate (approximated by the flux of mineral sediments) and biogeochemical sedimentary proxies for climate, permafrost, hydrology, soil, vegetation, and fire. We analyze the proxy data with a combination of bi- and multi-variate techniques, with sediment flux as the response variable, and the different biogeochemical sedimentary proxies as the predictors. The results are generally consistent between different analysis methods, and show that sediment flux is most strongly associated with temperature (mean July temperature based on Chironomid taxa) and vegetation-related proxies (normalized pollen counts and percent pollen sourced from trees and shrubs), and have a weaker, albeit statistically significant, association with proxies such as fire frequency, aeolian dust supply, age-offset, and geochemical indicators of mass wasting. The relations between erosion-rate and different sedimentary proxies are often noisy but are typically characterized by a consistent general trend. Sediment flux generally decreases with increased temperature, suggesting that increased temperature is associated with environmental changes that protect the landscape from erosion. Decreased sediment flux with increased vegetation-related proxies suggests that increased vegetation abundance and shrub expansion stabilize the landscape. The association between sediment flux and vegetation-related proxies, as well as hydrologic ( $\delta^{18}\text{O}$ ), grain size, and fire related proxies change abruptly across some threshold values, highlighting the potential for strong non-linear changes in erosion in response to future changes in Arctic conditions.

## Data Availability Statement

A table with the time series of the proxies used for the analysis is available in the supplementary data. Additional complementary data is available through: <https://www.ncsl.noaa.gov/access/paleo-search/study/15675>; <https://sites.pitt.edu/~mabbott1/climate/mark/Abstracts/Pubs/Finkenbinderetal15Data.xlsx>; <https://sites.pitt.edu/~mabbott1/climate/mark/Abstracts/Pubs/BurialLakeDataNOAA.xlsx>. Software for this research is available in these in-text citation references: “Boruta” (R) (Kursa & Rudnicki, 2010), “iml” (R) (Molnar, 2018) as well as in MATLAB'S statistics and machine learning toolbox (MATLAB, 2021).

## Acknowledgments

This research was supported by Grant No. 1841400 from the United States National Science Foundation (NSF) to ES and MA. The authors thank Dr. Ben Gaglioti and an anonymous reviewer for insightful and thorough comments that meaningfully improved this manuscript. ES thanks Drs. Joel Rowland and Umakant Mishra for valuable discussion about erosion in permafrost landscapes.

## References

- Abbott, M. B., Edwards, M. E., & Finney, B. P. (2010). A 40, 000-yr record of environmental change from Burial Lake in Northwest Alaska. *Quaternary Research*, 74(1), 156–165. <https://doi.org/10.1016/j.yqres.2010.03.007>
- Abbott, M. B., Finney, B. P., Edwards, M. E., & Kelts, K. R. (2000). Lake-Level reconstruction and paleohydrology of Birch Lake, Central Alaska, based on seismic reflection profiles and Core transects. *Quaternary Research*, 53(2), 154–166. <https://doi.org/10.1006/qres.1999.2112>
- Abbott, M. B., & Stafford, T. W. (1996). Radiocarbon geochemistry of modern and ancient Arctic lake systems, Baffin Island, Canada. *Quaternary Research*, 45(3), 300–311. <https://doi.org/10.1006/qres.1996.0031>
- Aliyuda, K., Howell, J., & Humphrey, E. (2020). Impact of geological variables in Controlling oil-reservoir performance: An insight from a machine-Learning technique. *SPE Reservoir Evaluation and Engineering*, 23(04), 1314–1327. <https://doi.org/10.2118/201196-pa>
- Anderson, R. S., & Anderson, S. P. (2010). *Geomorphology: The mechanics and chemistry of landscapes*. Cambridge University Press. <https://doi.org/10.1017/cbo9780511794827.018>
- Apley, D. W., & Zhu, J. (2020). Visualizing the effects of predictor variables in black box supervised learning models. *Journal of the Royal Statistical Society: Series B*, 82(4), 1059–1086. <https://doi.org/10.1111/rssb.12377>
- Atchley, A. L., Coon, E. T., Painter, S. L., Harp, D. R., & Wilson, C. J. (2016). Influences and interactions of inundation, peat, and snow on active layer thickness. *Geophysical Research Letters*, 43(10), 5116–5123. <https://doi.org/10.1002/2016gl068550>
- Balsler, A. W., Jones, J. B., & Jorgenson, M. T. (2016). Relationship of permafrost cryofacies to varying surface and subsurface terrain conditions in the Brooks Range and foothills of northern Alaska, USA. *The Cryosphere Discussions*, 1–50. <https://doi.org/10.5194/tc-2016-224>
- Baughman, C. A., Mann, D. H., Verbyla, D. L., & Kunz, M. L. (2015). Soil surface organic layers in Arctic Alaska: Spatial distribution, rates of formation, and microclimatic effects. *Journal of Geophysical Research: Biogeosciences*, 120(6), 1150–1164. <https://doi.org/10.1002/2015JG002983>
- Bilotta, G., & Brazier, R. (2008). Understanding the influence of suspended solids on water quality and aquatic biota. *Water Research*, 42(12), 2849–2861. <https://doi.org/10.1016/j.watres.2008.03.018>
- Bintanja, R., & Andry, O. (2017). Towards a rain-dominated Arctic. *Nature Climate Change*, 7(4), 263–267. <https://doi.org/10.1038/nclimate3240>
- Blaauw, M., & Christen, J. A. (2011). Flexible paleoclimate age-depth models using an autoregressive gamma process. *Bayesian analysis*, 6(3), 457–474. <https://doi.org/10.1017/rdc.2020.41>

- Blaauw, M., Christen, J. A., Lopez, M. A. A., Vazquez, J. E., Belding, T., Theiler, J., et al. (2021). Package 'rbacon'. <https://doi.org/10.7265/skbg-kf16>
- Bodmer, P., Wilkinson, J., & Lorke, A. (2020). Sediment properties drive spatial variability of potential methane production and oxidation in small streams. *Journal of Geophysical Research: Biogeosciences*, *125*(1). <https://doi.org/10.1029/2019jg005213>
- Bonfils, C., Phillips, T., Lawrence, D., Cameron-Smith, P., Riley, W., & Subin, Z. (2012). On the influence of shrub height and expansion on northern high latitude climate. *Environmental Research Letters*, *7*(1), 015503. <https://doi.org/10.1088/1748-9326/7/1/015503>
- Braig, E., Welzl, G., Stichler, W., Raeder, U., & Melzer, A. (2010). Entrainment, annual circulation and groundwater inflow in a chain of lakes as inferred by stable 18O isotopic signatures in the water column. *Journal of Limnology*, *69*(2), 278. <https://doi.org/10.4081/jlimnol.2010.278>
- Breiman, L. (2001). Random forests. *Machine Learning*, *45*(1), 5–32. <https://doi.org/10.1023/a:1010933404324>
- Carswell, W. J. (2013). The 3D elevation program: Summary for Alaska. *US Geological Survey*. <https://doi.org/10.3133/fs20133083>
- Cerda, A. (1999). Parent material and vegetation affect soil erosion in eastern Spain. *Soil Science Society of America Journal*, *63*(2), 362–368. <https://doi.org/10.2136/sssaj1999.03615995006300020014x>
- Chin, K. S., Lento, J., Culp, J. M., Lancelle, D., & Kokelj, S. V. (2016). Permafrost thaw and intense thermokarst activity decreases abundance of stream benthic macroinvertebrates. *Global Change Biology*, *22*(8), 2715–2728. <https://doi.org/10.1111/gcb.13225>
- Chipman, M., & Hu, F. (2017). Linkages among climate, fire, and thermoerosion in Alaskan tundra over the past three millennia. *Journal of Geophysical Research: Biogeosciences*, *122*(12), 3362–3377. <https://doi.org/10.1002/2017jg004027>
- Clark, P. U., Dyke, A. S., Shakun, J. D., Carlson, A. E., Clark, J., Wohlfarth, B., et al. (2009). The last glacial maximum. *Science*, *325*(5941), 710–714. <https://doi.org/10.1126/science.1172873>
- Cockburn, J. M., & Lamoureux, S. F. (2008a). Hydroclimate controls over seasonal sediment yield in two adjacent High Arctic watersheds. *Hydrological Processes: An International Journal*, *22*(12), 2013–2027. <https://doi.org/10.1002/hyp.6798>
- Cockburn, J. M., & Lamoureux, S. F. (2008b). Inflow and lake controls on short-term mass accumulation and sedimentary particle size in a high Arctic lake: Implications for interpreting varved lacustrine sedimentary records. *Journal of Paleolimnology*, *40*(3), 923–942. <https://doi.org/10.1007/s10933-008-9207-5>
- Cohen, J., Screen, J. A., Furtado, J. C., Barlow, M., Whittleston, D., Coumou, D., et al. (2014). Recent Arctic amplification and extreme mid-latitude weather. *Nature Geoscience*, *7*(9), 627–637. <https://doi.org/10.1038/ngeo2234>
- Costard, F., Gautier, E., Brunstein, D., Hammadi, J., Fedorov, A., Yang, D., & Dupeyrat, L. (2007). Impact of the global warming on the fluvial thermal erosion over the Lena River in Central Siberia. *Geophysical Research Letters*, *34*(14), L14501. <https://doi.org/10.1029/2007gl030212>
- Cotton, J. M., Cerling, T. E., Hoppe, K. A., Mosier, T. M., & Still, C. J. (2016). Climate, CO<sub>2</sub>, and the history of North American grasses since the Last glacial maximum. *Science Advances*, *2*(3). <https://doi.org/10.1126/sciadv.1501346>
- Domine, F., Barrere, M., & Morin, S. (2016). The growth of shrubs on high Arctic tundra at Bylot Island: Impact on snow physical properties and permafrost thermal regime. *Biogeosciences*, *13*(23), 6471–6486. <https://doi.org/10.5194/bg-13-6471-2016>
- Dorfman, J., Stoner, J., Finkenbinder, M., Abbott, M., Xuan, C., & St-Onge, G. (2015). A 37, 000-year environmental magnetic record of Aeolian dust deposition from Burial Lake, Arctic Alaska. *Quaternary Science Reviews*, *128*, 81–97. <https://doi.org/10.1016/j.quascirev.2015.08.018>
- Droppo, I. G., di Cenzo, P., McFadyen, R., & Reid, T. (2021). Assessment of the sediment and associated nutrient/contaminant continuum, from permafrost thaw slump scars to tundra lakes in the Western Canadian Arctic. *Permafrost and Periglacial Processes*, *33*(1), 32–45. <https://doi.org/10.1002/ppp.2134>
- Elmendorf, S. C., Henry, G. H. R., Hollister, R. D., Björk, R. G., Boulanger-Lapointe, N., Cooper, E. J., et al. (2012). Plot-scale evidence of tundra vegetation change and links to recent summer warming. *Nature Climate Change*, *2*(6), 453–457. <https://doi.org/10.1038/nclimate1465>
- Evans, S. G., Godsey, S. E., Rushlow, C. R., & Voss, C. (2020). Water tracks enhance water flow above permafrost in upland Arctic Alaska hillslopes. *Journal of Geophysical Research: Earth Surface*, *125*(2), e2019JF005256. <https://doi.org/10.1029/2019jef005256>
- Finkenbinder, M. S., Abbott, M., Finney, B., Stoner, J., & Dorfman, J. (2015). A multi-proxy reconstruction of environmental change spanning the last 37, 000 years from Burial Lake, Arctic Alaska. *Quaternary Science Reviews*, *126*, 227–241. <https://doi.org/10.1016/j.quascirev.2015.08.031>
- Finkenbinder, M. S., Abbott, M. B., Edwards, M. E., Langdon, C. T., Steinman, B. A., & Finney, B. P. (2014). A 31, 000 year record of paleoenvironmental and lake-level change from Harding Lake, Alaska, USA. *Quaternary Science Reviews*, *87*, 98–113. <https://doi.org/10.1016/j.quascirev.2014.01.005>
- Finkenbinder, M. S., Abbott, M. B., Stoner, J. S., Ortiz, J. D., Finney, B. P., Dorfman, J. M., & Stansell, N. D. (2018). Millennial-scale variability in Holocene aquatic productivity from Burial Lake, Arctic Alaska. *Quaternary Science Reviews*, *187*, 220–234. <https://doi.org/10.1016/j.quascirev.2018.03.019>
- Friedman, J. H. (2001). Greedy function approximation: A gradient boosting machine. *Annals of Statistics*, *29*(5), 1189–1232. <https://doi.org/10.1214/aos/1013203451>
- Fuchs, M., Nitze, I., Strauss, J., Günther, F., Wetterich, S., Kizyakov, A., et al. (2020). Rapid fluvio-thermal erosion of a yedoma permafrost cliff in the Lena River Delta. *Frontiers of Earth Science*, *8*(336). <https://doi.org/10.3389/feart.2020.00336>
- Gaglioti, B. V., Mann, D. H., Jones, B. M., Pohlman, J. W., Kunz, M. L., & Wooller, M. J. (2014). Radiocarbon age-offsets in an arctic lake reveal the long-term response of permafrost carbon to climate change. *Journal of Geophysical Research: Biogeosciences*, *119*(8), 1630–1651. <https://doi.org/10.1002/2014jg002688>
- Gaglioti, B. V., Mann, D. H., Wooller, M. J., Jones, B. M., Wiles, G. C., Groves, P., et al. (2017). Younger-Dryas cooling and sea-ice feedbacks were prominent features of the Pleistocene-Holocene transition in Arctic Alaska. *Quaternary Science Reviews*, *169*, 330–343. <https://doi.org/10.1016/j.quascirev.2017.05.012>
- Galkin, F., Aliper, A., Putin, E., Kuznetsov, I., Gladyshev, V. N., & Zhavoronkov, A. (2018). Human microbiome aging clocks based on deep learning and tandem of permutation feature importance and accumulated local effects. *bioRxiv*, 507780. <https://doi.org/10.1101/302011>
- Godin, E., & Fortier, D. (2012). Geomorphology of a thermo-erosion gully, Bylot Island, Nunavut, Canada. *Canadian Journal of Earth Sciences*, *49*(8), 979–986. <https://doi.org/10.1139/e2012-015>
- Godin, E., Fortier, D., & Coulombe, S. (2014). Effects of thermo-erosion gully on hydrologic flow networks, discharge and soil loss. *Environmental Research Letters*, *9*(10), 105010. <https://doi.org/10.1088/1748-9326/9/10/105010>
- Golden, L. A., & Springer, G. S. (2006). Channel geometry, median grain size, and stream power in small mountain streams. *Geomorphology*, *78*(1–2), 64–76. <https://doi.org/10.1016/j.geomorph.2006.01.031>
- Gooseff, M. N., Balsler, A., Bowden, W. B., & Jones, J. B. (2009). Effects of hillslope thermokarst in northern Alaska. *Eos, Transactions American Geophysical Union*, *90*(4), 29–30. <https://doi.org/10.1029/2009eo040001>
- Granger, C. W. J. (1969). Investigating Causal relations by econometric models and cross-spectral methods. *Econometrica*, *37*(3), 424. <https://doi.org/10.2307/1912791>
- Gyssels, G., Poesen, J., Bochet, E., & Li, Y. (2005). Impact of plant roots on the resistance of soils to erosion by water: A review. *Progress in Physical Geography*, *29*(2), 189–217. <https://doi.org/10.1191/0309133305pp443ra>



- Hamilton, T. D. (2001). Quaternary glacial, lacustrine, and fluvial interactions in the Western Noatak basin, Northwest Alaska. *Quaternary Science Reviews*, 20(1–3), 371–391. [https://doi.org/10.1016/s0277-3791\(00\)00110-4](https://doi.org/10.1016/s0277-3791(00)00110-4)
- Harden, J. W., Koven, C. D., Ping, C.-L., Hugelius, G., McGuire, A. D., Camill, P., et al. (2012). Field information links permafrost carbon to physical vulnerabilities of thawing. *Geophysical Research Letters*, 39(15). <https://doi.org/10.1029/2012gl051958>
- Heijmans, M. M., Magnússon, R. Í., Lara, M. J., Frost, G. V., Myers-Smith, I. H., van Huissteden, J., et al. (2022). Tundra vegetation change and impacts on permafrost. *Nature Reviews Earth & Environment*, 3(1), 68–84. <https://doi.org/10.1038/s43017-021-00233-0>
- Higuera, P. (2009). CharAnalysis 0.9: Diagnostic and analytical tools for sediment-charcoal analysis. In *User's guide*. Montana State University.
- Higuera, P. E., Barnes, J. L., Chipman, M., & Hu, F. S. (2011). The burning tundra: A look back at the last 6, 000 years of fire in the Noatak National Preserve, northwestern Alaska. *Alaska Park Sci*, 10, 36–41.
- Higuera, P. E., Brubaker, L. B., Anderson, P. M., Brown, T. A., Kennedy, A. T., & Hu, F. S. (2008). Frequent fires in ancient shrub tundra: Implications of paleorecords for Arctic environmental change. *PLoS One*, 3(3), e0001744. <https://doi.org/10.1371/journal.pone.0001744>
- Higuera, P. E., Chipman, M. L., Barnes, J. L., Urban, M. A., & Hu, F. S. (2011). Variability of tundra fire regimes in Arctic Alaska: Millennial-scale patterns and ecological implications. *Ecological Applications*, 21(8), 3211–3226. <https://doi.org/10.1890/11-0387.1>
- Hooker, G., Mentch, L., & Zhou, S. (2021). Unrestricted permutation forces extrapolation: Variable importance requires at least one more model, or there is no free variable importance. *Statistics and Computing*, 31(6), 82. <https://doi.org/10.1007/s11222-021-10057-z>
- Horton, R. E. (1945). Erosional development of streams and their drainage basins; hydrophysical approach to quantitative morphology. *The Geological Society of America Bulletin*, 56(3), 275–370. [https://doi.org/10.1130/0016-7606\(1945\)56\[275:edosat\]2.0.co;2](https://doi.org/10.1130/0016-7606(1945)56[275:edosat]2.0.co;2)
- Huh, Y., & Edmond, J. M. (1999). The fluvial geochemistry of the rivers of eastern Siberia: III. Tributaries of the Lena and Anabar draining the basement terrain of the Siberian craton and the trans-Baikal Highlands. *Geochimica et Cosmochimica Acta*, 63(7–8), 967–987. [https://doi.org/10.1016/s0016-7037\(99\)00045-9](https://doi.org/10.1016/s0016-7037(99)00045-9)
- Jenny, J.-P., Koirala, S., Gregory-Eaves, I., Francus, P., Niemann, C., Ahrens, B., et al. (2019). Human and climate global-scale imprint on sediment transfer during the Holocene. *Proceedings of the National Academy of Sciences*, 116(46), 22972–22976. <https://doi.org/10.1073/pnas.1908179116>
- Jerolmack, D. J., & Paola, C. (2010). Shredding of environmental signals by sediment transport. *Geophysical Research Letters*, 37(19). <https://doi.org/10.1029/2010gl044638>
- Jones, B. M., Grosse, G., Arp, C. D., Miller, E., Liu, L., Hayes, D. J., & Larsen, C. F. (2015). Recent Arctic tundra fire initiates widespread thermokarst development. *Scientific Reports*, 5(1), 1–13. <https://doi.org/10.1038/srep15865>
- Jones, M. C., & Yu, Z. (2010). Rapid deglacial and early Holocene expansion of peatlands in Alaska. *Proceedings of the National Academy of Sciences*, 107(16), 7347–7352. <https://doi.org/10.1073/pnas.0911387107>
- Jorgenson, M. T., Romanovsky, V., Harden, J., Shur, Y., O'Donnell, J., Schuur, E. A., et al. (2010). Resilience and vulnerability of permafrost to climate change. *Canadian Journal of Forest Research*, 40(7), 1219–1236. <https://doi.org/10.1139/x10-060>
- Kaufman, D. (2004). Holocene thermal maximum in the Western Arctic (0–180°W). *Quaternary Science Reviews*, 23(5–6), 529–560. <https://doi.org/10.1016/j.quascirev.2003.09.007>
- Kemsley, E. (1996). Discriminant analysis of high-dimensional data: A comparison of principal components analysis and partial least squares data reduction methods. *Chemometrics and Intelligent Laboratory Systems*, 33(1), 47–61. [https://doi.org/10.1016/0169-7439\(95\)00090-9](https://doi.org/10.1016/0169-7439(95)00090-9)
- King, A. L., Anderson, L., Abbott, M., Edwards, M., Finkenbinder, M. S., Finney, B., & Wooller, M. J. (2021). A stable isotope record of late Quaternary hydrologic change in the northwestern Brooks Range, Alaska (eastern Beringia). *Journal of Quaternary Science*. <https://doi.org/10.1002/jqs.3368>
- Kirkby, M. (1995). A model for variations in gelifluction rates with temperature and topography: Implications for global change. *Geografiska Annaler - Series A: Physical Geography*, 77(4), 269–278. <https://doi.org/10.1080/04353676.1995.11880447>
- Kociuba, W., & Janicki, G. (2015). Changeability of movable bed-surface particles in natural, gravel-bed channels and its relation to bedload grain size distribution (Scott River, Svalbard). *Geografiska Annaler - Series A: Physical Geography*, 97(3), 507–521. <https://doi.org/10.1111/geoa.12090>
- Kokelj, S. V., & Jorgenson, M. (2013). Advances in thermokarst research. *Permafrost and Periglacial Processes*, 24(2), 108–119. <https://doi.org/10.1002/ppp.1779>
- Konapala, G., & Mishra, A. (2020). Quantifying climate and catchment control on hydrological drought in the continental United States. *Water Resources Research*, 56(1). <https://doi.org/10.1029/2018wr024620>
- Kropp, H., Lorant, M. M., Natali, S. M., Kholodov, A. L., Rocha, A. V., Myers-Smith, I., et al. (2020). Shallow soils are warmer under trees and tall shrubs across arctic and boreal ecosystems. *Environmental Research Letters*, 16(1), 015001. <https://doi.org/10.1088/1748-9326/abc994>
- Kurek, J., Cwynar, L. C., Ager, T. A., Abbott, M. B., & Edwards, M. E. (2009). Late Quaternary paleoclimate of Western Alaska inferred from fossil Chironomids and its relation to vegetation histories. *Quaternary Science Reviews*, 28(9–10), 799–811. <https://doi.org/10.1016/j.quascirev.2008.12.001>
- Kursa, M. B. (2014). Robustness of Random Forest-based gene selection methods. *BMC Bioinformatics*, 15(1), 1–8. <https://doi.org/10.1186/1471-2105-15-8>
- Kursa, M. B., & Rudnicki, W. R. (2010). Feature selection with the Boruta Package. *Journal of Statistical Software*, 36(11). <https://doi.org/10.18637/jss.v036.i11>
- Lafrenière, M. J., & Lamoureux, S. F. (2019). Effects of changing permafrost conditions on hydrological processes and fluvial fluxes. *Earth-Science Reviews*, 191, 212–223. <https://doi.org/10.1016/j.earscirev.2019.02.018>
- Lamoureux, S. (2000). Five centuries of interannual sediment yield and rainfall-induced erosion in the Canadian High Arctic recorded in lacustrine varves. *Water Resources Research*, 36(1), 309–318. <https://doi.org/10.1029/1999wr900271>
- Lamoureux, S. F., Lafrenière, M. J., & Favaro, E. A. (2014). Erosion dynamics following localized permafrost slope disturbances. *Geophysical Research Letters*, 41(15), 5499–5505. <https://doi.org/10.1002/2014gl060677>
- Landers, D. H., Simonich, S. L., Jaffe, D. A., Geiser, L. H., Campbell, D. H., Schwindt, A. R., et al. (2008). *The fate, transport, and ecological impacts of airborne contaminants in western national parks (USA)*. Western Airborne Contaminants Assessment Project Final Report.
- Lane, S. N. (2012). 21st century climate change: Where has all the geomorphology gone? *Earth Surface Processes and Landforms*, 38(1), 106–110. <https://doi.org/10.1002/esp.3362>
- Lantz, T. C., & Kokelj, S. V. (2008). Increasing rates of retrogressive thaw slump activity in the Mackenzie Delta region, NWT, Canada. *Geophysical Research Letters*, 35(6), L06502. <https://doi.org/10.1029/2007gl032433>
- Lara, M. J., Chipman, M. L., & Hu, F. S. (2019). Automated detection of thermoerosion in permafrost ecosystems using temporally dense landsat image stacks. *Remote Sensing of Environment*, 221, 462–473. <https://doi.org/10.1016/j.rse.2018.11.034>
- Levenstein, B., Lento, J., & Culp, J. (2020). Effects of prolonged sedimentation from permafrost degradation on macroinvertebrate drift in Arctic streams. *Limnology & Oceanography*, 9999(S1), 1–12. <https://doi.org/10.1002/lno.11657>

- Lewkowicz, A. G., & Harris, C. (2005). Morphology and geotechnique of active-layer detachment failures in discontinuous and continuous permafrost, northern Canada. *Geomorphology*, 69(1–4), 275–297. <https://doi.org/10.1016/j.geomorph.2005.01.011>
- Li, D., Lu, X., Overeem, I., Walling, D. E., Syvitski, J., Kettner, A. J., et al. (2021). Exceptional increases in fluvial sediment fluxes in a warmer and wetter High Mountain Asia. *Science*, 374(6567), 599–603. <https://doi.org/10.1126/science.abi9649>
- Liljedahl, A. K., Boike, J., Daanen, R. P., Fedorov, A. N., Frost, G. V., Grosse, G., et al. (2016). Pan-Arctic ice-wedge degradation in warming permafrost and its influence on tundra hydrology. *Nature Geoscience*, 9(4), 312–318. <https://doi.org/10.1038/ngeo2674>
- Lin, W., & Wang, C. (2021). Longer summers in the Northern Hemisphere under global warming. *Climate Dynamics*, 58(9–10), 1–15. <https://doi.org/10.1007/s00382-021-06009-y>
- MacCumber, A. L., Patterson, R. T., Galloway, J. M., Falck, H., & Swindles, G. T. (2018). Reconstruction of Holocene hydroclimatic variability in subarctic treeline lakes using lake sediment grain-size end-members. *The Holocene*, 28(6), 845–857. <https://doi.org/10.1177/0959683617752836>
- Mann, D. H., Groves, P., Reanier, R. E., & Kunz, M. L. (2010). Floodplains, permafrost, cottonwood trees, and peat: What happened the last time climate warmed suddenly in arctic Alaska? *Quaternary Science Reviews*, 29(27–28), 3812–3830. <https://doi.org/10.1016/j.quascirev.2010.09.002>
- Mann, D. H., Peteet, D. M., Reanier, R. E., & Kunz, M. L. (2002). Responses of an arctic landscape to Lateglacial and early Holocene climatic changes: The importance of moisture. *Quaternary Science Reviews*, 21(8–9), 997–1021. [https://doi.org/10.1016/s0277-3791\(01\)00116-0](https://doi.org/10.1016/s0277-3791(01)00116-0)
- MATLAB. (2021). *Version 9.10.0 (R2021a)*. The MathWorks Inc.
- McCarty, J. L., Aalto, J., Paunu, V.-V., Arnold, S. R., Eckhardt, S., Klimont, Z., et al. (2021). Reviews and syntheses: Arctic fire regimes and emissions in the 21st century. *Biogeosciences*, 18(18), 5053–5083. <https://doi.org/10.5194/bg-18-5053-2021>
- Mehmoed, T., Liland, K. H., Snipen, L., & Sæbø, S. (2012). A review of variable selection methods in partial least squares regression. *Chemometrics and Intelligent Laboratory Systems*, 118, 62–69. <https://doi.org/10.1016/j.chemolab.2012.07.010>
- Meredith, M., Sommerkorn, M., Cassotta, S., Derksen, C., Ekaykin, A., Hollowed, A., et al. (2019). Polar Regions. Chapter 3, IPCC Special Report on the ocean and cryosphere in a changing climate. In *The ocean and cryosphere in a changing climate* (pp. 3–36). Cambridge University Press. <https://doi.org/10.1017/9781009157964.001>
- Meyers, P. A., & Teranes, J. L. (2002). Sediment organic matter. In *Tracking environmental change using lake sediments* (pp. 239–269). Springer. <https://doi.org/10.1007/0-306-47670-3>
- Molnar, C. (2018). iml: An R package for interpretable machine Learning. *Journal of Open Source Software*, 3(26), 786. <https://doi.org/10.21105/joss.00786>
- Murton, J. B., Goslar, T., Edwards, M. E., Bateman, M. D., Danilov, P. P., Savvinov, G. N., et al. (2015). Palaeoenvironmental interpretation of Yedoma silt (ice complex) deposition as cold-climate loess, Duvanny Yar, northeast Siberia. *Permafrost and Periglacial Processes*, 26(3), 208–288. <https://doi.org/10.1002/ppp.1843>
- Myers-Smith, I. H., Grabowski, M. M., Thomas, H. J. D., Angers-Blondin, S., Daskalova, G. N., Bjorkman, A. D., et al. (2019). Eighteen years of ecological monitoring reveals multiple lines of evidence for tundra vegetation change. *Ecological Monographs*, 89(2). <https://doi.org/10.1002/ecm.1351>
- Natali, S. M., Holdren, J. P., Rogers, B. M., Treharne, R., Duffy, P. B., Pomerance, R., & MacDonald, E. (2021). Permafrost carbon feedbacks threaten global climate goals. *Proceedings of the National Academy of Sciences*, 118(21). <https://doi.org/10.1073/pnas.2100163118>
- Nauta, A. L., Heijmans, M. M. P. D., Blok, D., Limpens, J., Elberling, B., Gallagher, A., et al. (2014). Permafrost collapse after shrub removal shifts tundra ecosystem to a methane source. *Nature Climate Change*, 5(1), 67–70. <https://doi.org/10.1038/nclimate2446>
- Nicodemus, K. K., Malley, J. D., Strobl, C., & Ziegler, A. (2010). The behaviour of random forest permutation-based variable importance measures under predictor correlation. *BMC Bioinformatics*, 11(1), 110. <https://doi.org/10.1186/1471-2105-11-110>
- O'Connor, M. T., Cardenas, M. B., Neilson, B. T., Nicholaides, K. D., & Kling, G. W. (2019). Active layer groundwater flow: The interrelated effects of stratigraphy, thaw, and topography. *Water Resources Research*, 55(8), 6555–6576. <https://doi.org/10.1029/2018wr024636>
- Olefeldt, D., Goswami, S., Grosse, G., Hayes, D., Hugelius, G., Kuhry, P., et al. (2016). Circumpolar distribution and carbon storage of thermokarst landscapes. *Nature Communications*, 7(1), 1–11. <https://doi.org/10.1038/ncomms13043>
- Osterkamp, T. E., Jorgenson, M. T., Schuur, E. A. G., Shur, Y. L., Kanevskiy, M. Z., Vogel, J. G., & Tumskey, V. E. (2009). Physical and ecological changes associated with warming permafrost and thermokarst in Interior Alaska. *Permafrost and Periglacial Processes*, 20(3), 235–256. <https://doi.org/10.1002/ppp.656>
- Palmtag, J., Hugelius, G., Lashchinskiy, N., Tamstorf, M. P., Richter, A., Elberling, B., & Kuhry, P. (2015). Storage, landscape distribution, and burial history of soil organic matter in contrasting areas of continuous permafrost. *Arctic Antarctic and Alpine Research*, 47(1), 71–88. <https://doi.org/10.1657/aaar0014-027>
- Patton, A. I., Rathburn, S. L., & Capps, D. M. (2019). Landslide response to climate change in permafrost regions. *Geomorphology*, 340, 116–128. <https://doi.org/10.1016/j.geomorph.2019.04.029>
- Payne, C., Panda, S., & Prakash, A. (2018). Remote sensing of river erosion on the colville river, north slope Alaska. *Remote Sensing*, 10(3), 397. <https://doi.org/10.3390/rs10030397>
- Pelletier, J. D., Brad Murray, A., Pierce, J. L., Bierman, P. R., Breshears, D. D., Crosby, B. T., et al. (2015). Forecasting the response of earth's surface to future climatic and land use changes: A review of methods and research needs. *Earth's Future*, 3(7), 220–251. <https://doi.org/10.1002/2014ef000290>
- Pelletier, J. D., Broxton, P. D., Hazenberg, P., Zeng, X., Troch, P. A., Niu, G.-Y., et al. (2016). A gridded global data set of soil, intact regolith, and sedimentary deposit thicknesses for regional and global land surface modeling. *Journal of Advances in Modeling Earth Systems*, 8(1), 41–65. <https://doi.org/10.1002/2015ms000526>
- Qin, F., Bunting, M. J., Zhao, Y., Li, Q., Cui, Q., & Ren, W. (2020). Relative pollen productivity estimates for alpine meadow vegetation, north-eastern Tibetan Plateau. *Vegetation History and Archaeobotany*, 29(4), 447–462. <https://doi.org/10.1007/s00334-019-00751-4>
- Rafat, A., Rezanezhad, F., Quinton, W. L., Humphreys, E. R., Webster, K., & Cappellen, P. V. (2021). Non-growing season carbon emissions in a northern peatland are projected to increase under global warming. *Communications Earth & Environment*, 2(1), 111. <https://doi.org/10.1038/s43247-021-00184-w>
- Reimer, P. J., Austin, W. E. N., Bard, E., Bayliss, A., Blackwell, P. G., Ramsey, C. B., et al. (2020). The IntCal20 Northern Hemisphere radiocarbon Age Calibration Curve (0–55 cal kBP). *Radiocarbon*, 62(4), 725–757. <https://doi.org/10.1017/rdc.2020.41>
- Romanovsky, V., & Osterkamp, T. (1997). Thawing of the active layer on the coastal plain of the Alaskan Arctic. *Permafrost and Periglacial Processes*, 8(1), 1–22. [https://doi.org/10.1002/\(sici\)1099-1530\(199701\)8:1](https://doi.org/10.1002/(sici)1099-1530(199701)8:1)
- Rowland, J., Jones, C., Altmann, G., Bryan, R., Crosby, B., Hinzman, L., et al. (2010). Arctic landscapes in transition: Responses to thawing permafrost. *Eos, Transactions American Geophysical Union*, 91(26), 229–230. <https://doi.org/10.1029/2010eo260001>
- Ryb, U., Matmon, A., Erel, Y., Haviv, I., Katz, A., Starinsky, A., et al. (2014). Controls on denudation rates in tectonically stable mediterranean carbonate terrain. *The Geological Society of America Bulletin*, 126(3–4), 553–568. <https://doi.org/10.1130/b30886.1>

- Sadler, P. M. (1981). Sediment Accumulation rates and the completeness of stratigraphic sections. *The Journal of Geology*, 89(5), 569–584. <https://doi.org/10.1086/628623>
- Salgado-Labouriau, M. L., & Rull, V. (1986). A method of introducing exotic pollen for paleoecological analysis of sediments. *Review of Palaeobotany and Palynology*, 47(1–2), 97–103. [https://doi.org/10.1016/0034-6667\(86\)90008-4](https://doi.org/10.1016/0034-6667(86)90008-4)
- Schädel, C., Bader, M. K.-F., Schuur, E. A., Biasi, C., Bracho, R., Čapek, P., et al. (2016). Potential carbon emissions dominated by carbon dioxide from thawed permafrost soils. *Nature Climate Change*, 6(10), 950–953. <https://doi.org/10.1038/nclimate3054>
- Schumm, S. A. (1979). Geomorphic thresholds: The concept and its applications. *Transactions of the Institute of British Geographers*, 4(4), 485–515. <https://doi.org/10.4324/9781003028697-22>
- Schuur, E. A. G., Bockheim, J., Canadell, J. G., Euskirchen, E., Field, C. B., Goryachkin, S. V., et al. (2008). Vulnerability of permafrost carbon to climate change: Implications for the global carbon cycle. *BioScience*, 58(8), 701–714. <https://doi.org/10.1641/b580807>
- Shelef, E., Rowland, J. C., Wilson, C. J., Hilley, G. E., Mishra, U., Altmann, G. L., & Ping, C.-L. (2017). Large uncertainty in permafrost carbon stocks due to hillslope soil deposits. *Geophysical Research Letters*, 44(12), 6134–6144. <https://doi.org/10.1002/2017gl073823>
- Spencer, T., & Lane, S. N. (2016). Reflections on the IPCC and global change science: Time for a more (physical) geographical tradition. *Canadian Geographer / Le Géographe Canadien*, 61(1), 124–135. <https://doi.org/10.1111/cag.12332>
- Stein, L., Clark, M. P., Knoben, W. J., Pianosi, F., & Woods, R. A. (2021). How do climate and catchment attributes influence flood generating processes? A large-sample study for 671 catchments across the contiguous USA. *Water Resources Research*, 57(4), e2020WR028300. <https://doi.org/10.1029/2020wr028300>
- Strunk, A., Olsen, J., Sanei, H., Rudra, A., & Larsen, N. K. (2020). Improving the reliability of bulk sediment radiocarbon dating. *Quaternary Science Reviews*, 242, 106442. <https://doi.org/10.1016/j.quascirev.2020.106442>
- Sugita, S. (2007). Theory of quantitative reconstruction of vegetation II: All you need is LOVE. *The Holocene*, 17(2), 243–257. <https://doi.org/10.1177/09595683607075838>
- Sun, W., Mu, X., Gao, P., Zhao, G., Li, J., Zhang, Y., & Chiew, F. (2019). Landscape patches influencing hillslope erosion processes and flow hydrodynamics. *Geoderma*, 353, 391–400. <https://doi.org/10.1016/j.geoderma.2019.07.003>
- Tape, K. D., Verbyla, D., & Welker, J. M. (2011). Twentieth century erosion in Arctic Alaska foothills: The influence of shrubs, runoff, and permafrost. *Journal of Geophysical Research*, 116(G4), G04024. <https://doi.org/10.1029/2011jg001795>
- Toniolo, H., Kodial, P., Hinzman, L., & Yoshikawa, K. (2009). Spatio-temporal evolution of a thermokarst in Interior Alaska. *Cold Regions Science and Technology*, 56(1), 39–49. <https://doi.org/10.1016/j.coldregions.2008.09.007>
- Trochim, E., Prakash, A., Kane, D., & Romanovsky, V. (2016). Remote sensing of water tracks. *Earth and Space Science*, 3(3), 106–122. <https://doi.org/10.1002/2015ea000112>
- Turetsky, M. R., Abbott, B. W., Jones, M. C., Anthony, K. W., Olefeldt, D., Schuur, E. A. G., et al. (2019). Permafrost collapse is accelerating carbon release. *Nature*, 569(7754), 32–34. <https://doi.org/10.1038/d41586-019-01313-4>
- Turetsky, M. R., Abbott, B. W., Jones, M. C., Anthony, K. W., Olefeldt, D., Schuur, E. A. G., et al. (2020). Carbon release through abrupt permafrost thaw. *Nature Geoscience*, 13(2), 138–143. <https://doi.org/10.1038/s41561-019-0526-0>
- Vachula, R. S., Huang, Y., Russell, J. M., Abbott, M. B., Finkenbinder, M. S., & O'Donnell, J. A. (2020). Sedimentary biomarkers reaffirm human impacts on northern beringian ecosystems during the last glacial period. *Boreas*, 49(3), 514–525. <https://doi.org/10.1111/bor.12449>
- van Huissteden, J. (2020). *Thawing permafrost*. Springer International Publishing. <https://doi.org/10.1007/978-3-030-31379-1>
- Vaughan, A. A., Belmont, P., Hawkins, C. P., & Wilcock, P. (2017). Near-channel versus watershed controls on sediment rating curves. *Journal of Geophysical Research: Earth Surface*, 122(10), 1901–1923. <https://doi.org/10.1002/2016jg004180>
- Vonk, J. E., Alling, V., Rahm, L., Mörth, C.-M., Humborg, C., & Gustafsson, Ö. (2012). A centennial record of fluvial organic matter input from the discontinuous permafrost catchment of Lake Torneträsk. *Journal of Geophysical Research*, 117(G3). <https://doi.org/10.1029/2011jg001887>
- Vucic, J. M., Gray, D. K., Cohen, R. S., Syed, M., Murdoch, A. D., & Sharma, S. (2020). Changes in water quality related to permafrost thaw may significantly impact zooplankton in small Arctic lakes. *Ecological Applications*, 30(8), e02186. <https://doi.org/10.1002/eap.2186>
- Weltje, G. J., & Tjallingii, R. (2008). Calibration of xrf core scanners for quantitative geochemical logging of sediment cores: Theory and application. *Earth and Planetary Science Letters*, 274(3–4), 423–438. <https://doi.org/10.1016/j.epsl.2008.07.054>
- Whitlock, C., & Larsen, C. (2002). Charcoal as a fire Proxy. In *Tracking environmental change using lake sediments* (pp. 75–97). Springer Netherlands. [https://doi.org/10.1007/0-306-47668-1\\_5](https://doi.org/10.1007/0-306-47668-1_5)
- Wijeyakulasuriya, D. A., Eisenhauer, E. W., Shaby, B. A., & Hanks, E. M. (2020). Machine learning for modeling animal movement. *PLoS One*, 15(7), e0235750. <https://doi.org/10.1371/journal.pone.0235750>
- Wilcox, E. J., Keim, D., de Jong, T., Walker, B., Sonnentag, O., Sniderhan, A. E., et al. (2019). Tundra shrub expansion may amplify permafrost thaw by advancing snowmelt timing. *Arctic Science*, 5(4), 202–217. <https://doi.org/10.1139/as-2018-0028>
- Woo, M.-K. (1983). Hydrology of a drainage basin in the Canadian high Arctic. *Annals of the Association of American Geographers*, 73(4), 577–596. <https://doi.org/10.1111/j.1467-8306.1983.tb01860.x>
- Woo, M.-K., & Sauriol, J. (1980). Channel development in snow-filled valleys, Resolute, NWT, Canada. *Geografiska Annaler - Series A: Physical Geography*, 62(1–2), 37–56. <https://doi.org/10.2307/520451>
- Xenochristou, M., Hutton, C., Hofman, J., & Kapelan, Z. (2021). Short-term forecasting of household water demand in the UK using an interpretable machine learning approach. *Journal of Water Resources Planning and Management*, 147(4), 04021004. [https://doi.org/10.1061/\(asce\)wr.1943-5452.0001325](https://doi.org/10.1061/(asce)wr.1943-5452.0001325)
- Yi, S., Woo, M.-k., & Arain, M. A. (2007). Impacts of peat and vegetation on permafrost degradation under climate warming. *Geophysical Research Letters*, 34(16). <https://doi.org/10.1029/2007gl030550>
- Zimov, S. A., Schuur, E. A., & Chapin, F. S., III. (2006). Permafrost and the global carbon budget. *Science (Washington D C)*, 312(5780), 1612–1613. <https://doi.org/10.1126/science.1128908>